NASA-CR-174647

R84AEB380

NASA

National Aeronautics and
Space Administration

EXTENDED PARAMETRIC REPRESENTATION OF COMPRESSOR FANS AND TURBINES

Volume III - MODFAN User's Manual

FINAL REPORT

March 1984

By

General Electric Company
Aircraft Engine Business Group
Advanced Technology Programs Dept.
Cincinnati, Ohio 45215

FOR

NATIONAL AERONAUTICS AND SPACE ADMINISTRATION
LEWIS RESEARCH CENTER
21000 BROOKPARK ROAD
CLEVELAND, OHIO 44135

Contract
NAS3-23055

GENERAL ELECTRIC

Aircraft Engine Business Group
Advanced Technology Programs Department
Cincinnati, Ohio 45215

1. Report No.	2. Government Accession No.	3. Recipient's Catalog No.
NASA CR-174647		

4. Title and Subtitle	5. Report Date
Extended Parametric Representation of Compressor Fans and Turbines Vol. III - MODFAN USER'S Manual (Parametric Modulating Flow Fan)	March 1984
	6. Performing Organization Code
7. Author(s)	8. Performing Organization Report No.
G.L. Converse	R84AEB380
	10. Work Unit No.
9. Performing Organization Name and Address	11. Contract or Grant No.
General Electric Company Aircraft Engine Business Group Cincinnati, Ohio 45215	NAS3-23055
12. Sponsoring Agency Name and Address	13. Type of Report and Period Covered
National Aeronautics and Space Administration Washington, D.C. 20546	Contract Report August 1982 - October 1983
	14. Sponsoring Agency Code

15. Supplementary Notes

Project Manager, James W. Gauntner, Aerospace Engineer, NASA Lewis Research Center, Cleveland, Ohio

16. Abstract

A modeling technique for single stage flow modulating fans or centrifugal compressors has been developed which will enable the user to obtain consistend and rapid off-design performance from design point input. The fan flow modulation may be obtained by either a VIGV (variable inlet guide vane) or a VPF (variable pitch rotor) option. Only the VIGV option is available for the centrifugal compressor. The modeling technique has been incorporated into a time-sharing program to facilitate its use. Because this report contains a description of the input output data, values of typical inputs, and example cases, it is suitable as a user's manual. This report is the last of a three volume set describing the parametric representation of compressor fans, and turbines. The titles of the three volumes are given below:

(1) Volume I CMGEN USER's Manual (Parametric Compressor Generator)
(2) Volume II PART USER's Manual (Parametric Turbine)
(3) Volume III MODFAN USER's Manual (Parametric Modulating Flow Fan)

17. Key Words (Suggested by Author(s))	18. Distribution Statement
Parametric Fans Parametric Centrifugal Compressors Off-Design Performance Flow Modulation	[redacted]

19. Security Classif. (of this report)	20. Security Classif. (of this page)	21. No. of Pages	22. Price*
Unclassified	Unclassified	50	

[redacted]

NASA-C-168 (Rev. 10-75)

TABLE OF CONTENTS

LIST OF FIGURES

1.0 INTRODUCTION

The NASA Lewis Research Center employs a general computer program NNEP (Ref.1) for calculating the thermodynamic performance of jet propulsion engines. To calculate off-design engine performance, the NNEP user must input component maps defining the characteristics of the various components over their full range of operating conditions.

For early cycle analysis of advanced propulsion systems, these map characteristics are not generally known because the geometry of the component has not been specified. Furthermore, the typical user of NNEP is not sufficiently knowledgeable and/or cannot afford the time to do an extensive design followed by an off-design analysis of the component in question to define the map characteristics. Typically, in this early stage, the user scales some available map.

The available methods for scaling maps can lead to significant errors in component representations. A traditional method of scaling a compressor map retains the flow speed relation of the base map and applies a constant pressure rise scalar calculated at the design point. Size scaling is, of course, legitimate. The accuracy of such a procedure can be considerably improved by using parametrically generated component maps. A parametric component representation can be thought of as a scaling procedure which uses the key design point parameters to impact the fundamental differences in the map characteristics when generating the component maps.

The objective of the present study is an improved method of representing single stage flow modulating fans and/or compressors of either the axial or centrifugal types when performing calculations of off-design performance for advanced air-breathing jet engines. The axial flow machines include flow modulation through either variable inlet guide vanes (VIGV) or variable rotor pitch (VPF). The centrifugal compressors include only the variable inlet guide vane (VIGV) option. This method, which is a computer program called MODFAN (i.e., flow modulating fan) is compatible in both form and format with the cycle program of Reference 1 and the example map representation of Reference 2.

This report is a user's manual for the computer program MODFAN and contains a description of the input-output data, values of typical inputs, and sample cases. A brief description of the engineering analysis used to generate a program is given near the end of the report.

The program uses design point data and semi-empirical correlations to generate off-design values of corrected flow,efficiency, and pressure ratio over a range of blade angles, corrected speeds, and pressure ratio parameters specified by the user.

2.0 PROGRAM STRUCTURE

A flow chart showing the flow of control in the MODFAN program is shown in Figure 1. The program first displays a description of the design point variables together with the default values. The user can then change the default values as desired. The input is then checked and the updated input displayed. This completes the input phase of the program. The design point calculations are then carried out. These calculations determine the blade row overall geometries from the design point input.

Once the design point calculations have been completed, the off-design calculation can begin. The calculations for each of the desired angles, speeds, and *R values are carried out in a set of nested DO loops. For each angle and speed, the min-loss point (i.e., the map backbone) is first located. Then the values of work coefficient both at stall and at a pressure ratio of unity are determined. These values of work coefficient form the upper and lower limits of the speed line. The R values are then converted into equivalent work coefficient values, and the fan characteristics determined. When the inner or R DO loop is completed the speed is incremented and the calculation repeated; when all speeds are completed, the angle is incremented.

After the off-design calculation has been completed, MODFAN writes the three data sets required for the computer program NNEP input.

*R is a measure of the relative distance along a speed line starting from R=1 at stall.

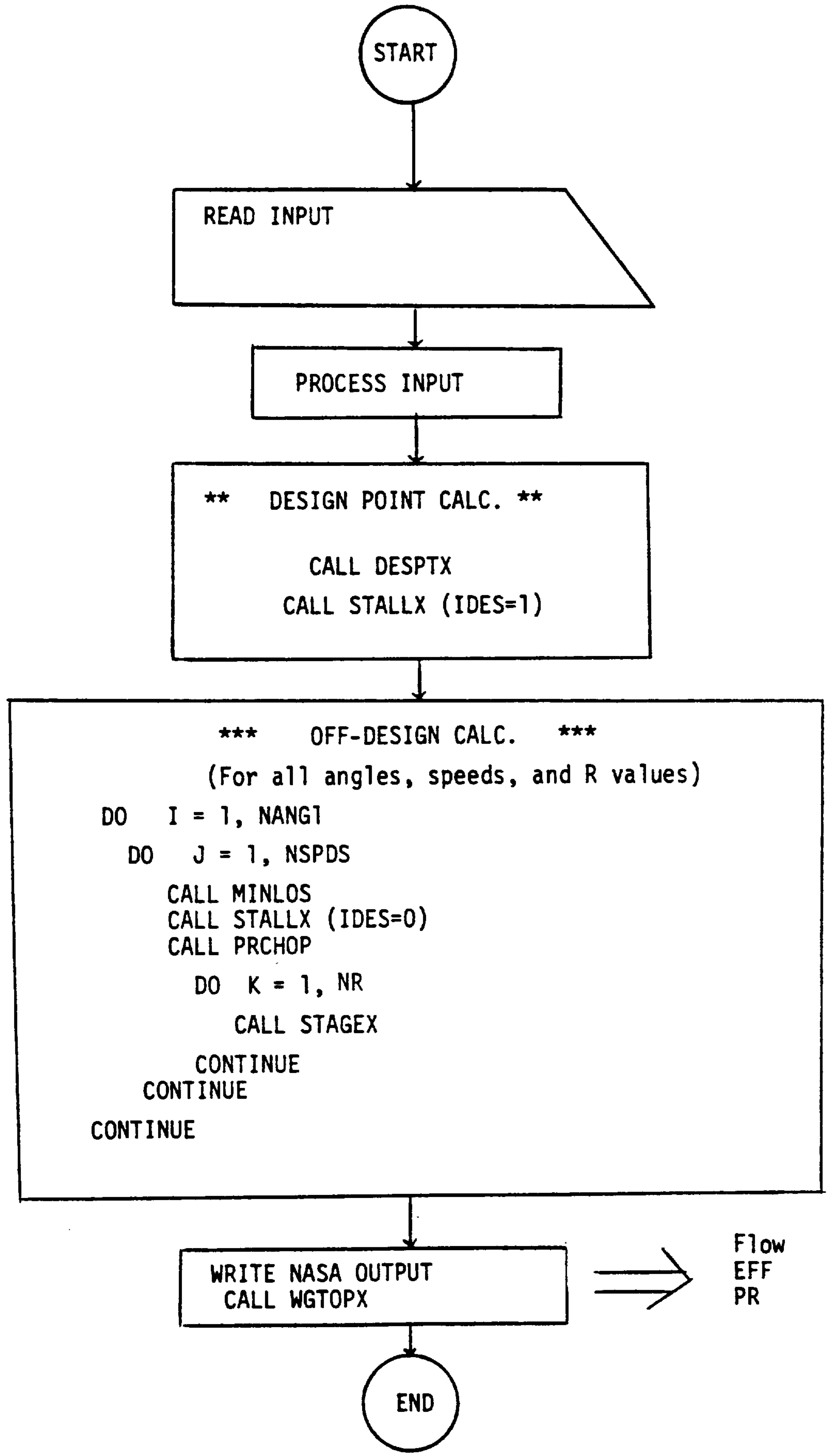

FIGURE 1. FLOW CHART SHOWING FLOW OF CONTROL IN MODFAN

3.0 PROGRAM INPUTS

Most of the MODFAN inputs are of the free-field format (NAMELIST) type, and begin in column two. The only exception is the initial type switch which requires either a 1 or 0 as a response. The program first gives a brief description of the variables used in the NAMELIST INPUT. The default settings of these variables are then displayed. The user can then enter changes in the design point values and/or the range of angle settings, speeds, and R values desired. If the user wishes the program to generate a value for the design point efficiency, a zero value should be input for EFFD. The program will then echo the updated NAMELIST and go into execution. Upon completion, the program will display a message to the effect that the NASA output files have been written on file codes 30, 31, and 32.

A sample of this showing the terminal conversation is shown in Figure 2 . This example is for a axial flow fan having fixed geometry. Note that all of the design point values have been reset as well as the range of inlet guide vane angles and corrected speeds. The range of R values has not been altered. The R values are used to fix a point on a speed line. The R value is unity at the stall line and increases along a constant speed line as the flow increases. The algorithm used in MODFAN forces a value of R equal to two at the min-loss point which is slightly below the peak efficiency on the speed line. The concept of min-loss is discussed in detail in Reference 3 .

The fan map generated by the program from the input values given in Figure 2 is shown in Figure 3. The locus of the R=1 and R=2 lines have been indicated on the figure.

```
************PARAMETRIC FLOW MODULATING FAN************

                    *M*O*D*F*A*N*

AXIAL OR CENT COMPRESSOR? 1=CENT;Ø OR CR=AXIAL
=Ø

DESCRIPTION OF INPUT VARIABLES IN MODFAN PROGRAM
(NAMELIST INPUT)

ITYPE=1       VIGV
ITYPE=2       VPF(NO IGV )

DESIGN POINT VALUES OF:

PQPD         PRESSURE RATIO(TOTAL-TO-TOTAL)
EFFD         ADIABATIC EFFICIENCY(TOTAL-TO TOTAL)
W1D          INLET CORRECTED FLOW
PSID         ROTOR EXIT MERIDIONAL LOADING(2GJ*DH/U2**2)
WQA1D        INLET CORRECTED FLOW PER UNIT AREA
XMZ2D        MERIDIONAL MACH NO AT ROTOR EXIT
SMD          CONSTANT SPEED STALL MARGIN(PERCENT)
STP1D        IGV METAL ANGLE

GEOMETRY SPECIFICATIONS

A3QA2        STATOR INLET TO ROTOR EXIT AREA RATIO
RRAT         INLET HUB TO TIP RADIUS RATIO
ROQI         RATIO OF ROTOR EXIT TO INLET RADII (MERIDIONAL LINE)

MAP RANGE (ARRAY VALUES MUST BE IN ASCENDING ORDER)

NR           NO OF R VALUES TO BE CALCULATED
AR           ARRAY OF R VALUES(1=STALL,2=MIN-LOSS)
NSPDS        NO OF SPEED LINES
APCNC        ARRAY OF SPEEDS (DECIMAL PERCENT)
NSTP1        NO OF IGV SETTINGS
ASTP1        ARRAY OF IGV ANGLES(-1Ø TO 4Ø DEG)
NROT1        NO OF ROTOR PITCH SETTINGS
AROT1        ARRAY OF ROTOR PITCH ANGLES( -5 TO 5 DEG)


 NAMELIST       INPUT
 ITYPE  =          1,
 PQPD   =     1.655Ø,     EFFD   =     Ø.834Ø,
 W1D    =   223.8ØØØ,     PSID   =     Ø.8226,
 WQA1D  =    41.Ø7ØØ,     XMZ2D  =     Ø.45ØØ,
 SMD    =    14.1ØØØ,     STP1D  =     Ø.    ,
 A3QA2  =     Ø.96ØØ,     RRAT   =     Ø.5ØØØ,
 ROQI   =     1.ØØØØ,
 NR     =         11
 AR(I)      =
     1         1.ØØØØ,        1.2ØØØ,        1.4ØØØ,        1.6ØØØ,
     5         1.8ØØØ,        2.ØØØØ,        2.2ØØØ,        2.4ØØØ,
     9         2.6ØØØ,        2.8ØØØ,        3.ØØØØ,
```

Figure 2. MODFAN Sample Terminal Conversation.

ORIGINAL PAGE IS
OF POOR QUALITY

```
 NSPDS =        6
 APCNC(I) =
     1      Ø.5ØØØ,     Ø.7ØØØ,     Ø.8ØØØ,     Ø.9ØØØ,
     5      1.ØØØØ,     1.1ØØØ,
 NSTP1 =        3
 ASTP1(I) =
     1      Ø.    ,    2Ø.ØØØØ,    4Ø.ØØØØ,
 NROT1 =        Ø
 AROT1(I) =
     1      Ø.    ,
 END NAMELIST      INPUT
ENTER CHANGES TO NAMELIST INPUT
=$INPUT NSTP1/ASTP1=Ø.Ø,
=PQPD=1.62,EFFD=.84,WQA1D=4Ø.Ø,W1D=219.2,PSID=.863,
=XMZ2D=.5,SMD=2Ø.Ø,STP1D=Ø.Ø,A3QA2=1.Ø5,RRAT=.5,ROQI=1.Ø,
=NSPDS/APCNC=.5,.7,.9,1.Ø,1.1,
=$

 NAMELIST      INPUT
 ITYPE =          1,
 PQPD  =     1.62ØØ,    EFFD   =    Ø.84ØØ,
 W1D   =   219.2ØØØ,    PSID   =    Ø.863Ø,
 WQA1D =    4Ø.ØØØØ,    XMZ2D  =    Ø.5ØØØ,
 SMD   =    2Ø.ØØØØ,    STP1D  =    Ø.    ,
 A3QA2 =     1.Ø5ØØ,    RRAT   =    Ø.5ØØØ,
 ROQI  =     1.ØØØØ,
 NR    =         11
 AR(I)    =
     1      1.ØØØØ,     1.2ØØØ,     1.4ØØØ,     1.6ØØØ,
     5      1.8ØØØ,     2.ØØØØ,     2.2ØØØ,     2.4ØØØ,
     9      2.6ØØØ,     2.8ØØØ,     3.ØØØØ,
 NSPDS =        5
 APCNC(I) =
     1      Ø.5ØØØ,     Ø.7ØØØ,     Ø.9ØØØ,     1.ØØØØ,
     5      1.1ØØØ,
 NSTP1 =        1
 ASTP1(I) =
     1      Ø.    ,
 NROT1 =        Ø
 AROT1(I) =
     1      Ø.    ,
 END NAMELIST      INPUT
OUTPUT ON IFC=3Ø,31,32

PROGRAM COMPLETE  &
```

Figure 2. MODFAN Sample Terminal Conversation (Continued).

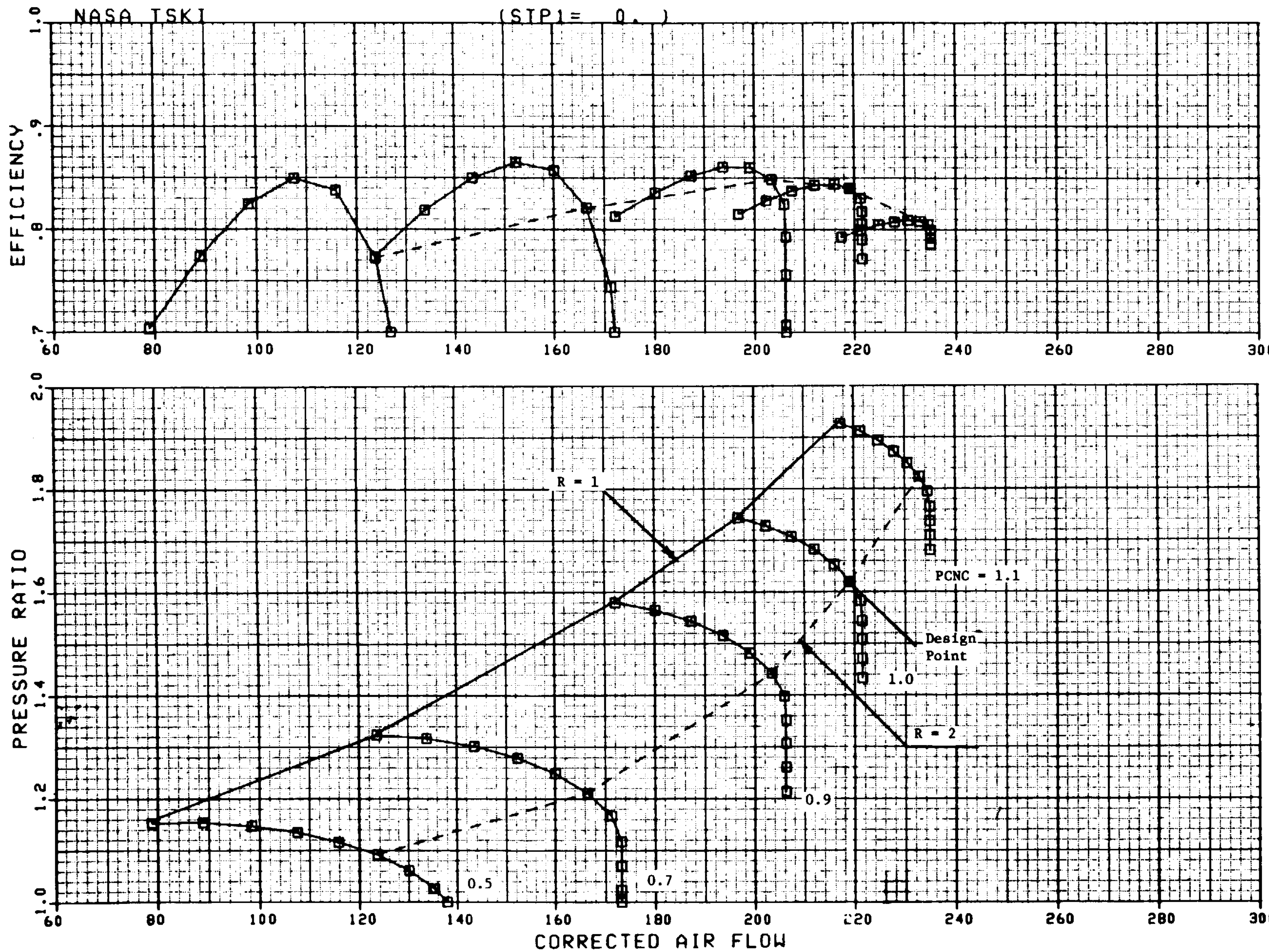

Figure 3. Parametric Fan Performance Map (PR = 1.6).

4.0 PROGRAM OUTPUTS

The basic output from the program consists of three tables. These tables show the variation in corrected flow, efficiency, and pressure ratio for each of the vane or rotor angles, R-values, and corrected speeds specified in the input. The output tables for the default cases are shown on pages 15 thru 17 and 20 thru 22. The table structure is compatible with NASA cycle deck requirements given in Reference 2 (pages 23 and 24).

The output tables can be visualized as three dimensional, composed of a series of planes with each plane assigned a value of angle position, STP1 or ROT1. Then in each angle plane, the dependent variable (ordinate axis) is a function of corrected speed, SPED, and R value. The dependent variables are respectively corrected flow, total-to-total efficiency, and pressure ratio.

For example, in the output table on page 20 the 12 lines of the dependent variable correspond to the 6 values of corrected speed, two lines per speed. Within each speed there are 11 R values.

It should be noted that for pressure ratios less than unity the efficiency is negative. These efficiency values are not incorrect, however, the efficiency behavior in this region makes curve fitting and interpolation of efficiency values extremely difficult. For this reason many engine manufactures use some form of locus or temperature ratio parameter rather than efficiency for interpolation. The solution used here was to simply discard the information below unity pressure ratio and to display the solution for unity pressure ratio for all values of R at which the pressure ratio is less than unity. This means that identical values of pressure ratio (PR=1.0), flow and efficiency (EFF=0.0) will appear in the output table on any speed line where the value of R results in a pressure ratio less than unity.

5.0 PROGRAM DIAGNOSTICS

The MODFAN computer program contains error printouts to aid the user in trouble shooting. A list of the error messages and their meaning are given below.

ERROR IN SUBROUTINE MINLOS.
PCN = F7.3, STP1 = F7.3, ROT1 = F7.3, ERR = F7.4

Failure to find the min-loss or "backbone location" at the input corrected speed and angle. The rotor is not choked.

ERROR IN SUBROUTINE ROTORC
TANA1 = F7.3, PCN = F7.3, PSI2J = F7.3, ERR = F7.4

Failure in the Newton-Raphson loop which solve the continuity equation across the rotor for the case where the rotor is choked.

NO STALL INTERSECTION FOUND: PCN = F7.2

Failure in the STALLX Subroutine. No stall intersection found at the specified speed and $\psi > 2$.

There are three iterations in the program which are balanced using the Method of False Position. This method is contained in the subroutine QIREXX. A maximum of 25 passes is allowed for any single iteration to balance. If the iteration does not balance within the specified tolerance the error message shown below will printout with the number of the offending iteration in the I5 format field.

QIRE CTR ERROR - - (CALLING LINE = I5)

QIRE LOOP	CALLING ROUTINE	COMMENTS
1	MINLOS	Calculation of Min-Loss or "Backbone" location at the input corrected speed and angle with Rotor choked.
2	STALLX	Calculation of the intersection of speed line and stall line (R=1).
3	PRCHOP	Calculation of the corrected flow at unity pressure ratio.

6.0 EXAMPLE CASES

Two example cases are given in order to illustrate the use of the program. The first case utilizes the default settings to generate a single stage fan having variable inlet guide vanes (VIGV). The second case uses the default settings to generate a single stage fixed geometry centrifugal compressor.

A complete record of the two terminal sessions including a listing of the output tables is given on the following pages. The program inputs and outputs have been discussed previously in Sections 3.0 and 4.0.

```
*************PARAMETRIC FLOW MODULATING FAN*************

                    *M*O*D*F*A*N*

AXIAL OR CENT COMPRESSOR? 1=CENT;Ø OR CR=AXIAL
=Ø

DESCRIPTION OF INPUT VARIABLES IN MODFAN PROGRAM
(NAMELIST INPUT)

ITYPE=1      VIGV
ITYPE=2      VPF(NO IGV )

DESIGN POINT VALUES OF:

PQPD         PRESSURE RATIO(TOTAL-TO-TOTAL)
EFFD         ADIABATIC EFFICIENCY(TOTAL-TO TOTAL)
W1D          INLET CORRECTED FLOW
PSID         ROTOR EXIT MERIDIONAL LOADING(2GJ*DH/U2**2)
WQA1D        INLET CORRECTED FLOW PER UNIT AREA
XMZ2D        MERIDIONAL MACH NO AT ROTOR EXIT
SMD          CONSTANT SPEED STALL MARGIN(PERCENT)
STP1D        IGV METAL ANGLE

GEOMETRY SPECIFICATIONS

A3QA2        STATOR INLET TO ROTOR EXIT AREA RATIO
RRAT         INLET HUB TO TIP RADIUS RATIO
ROQI         RATIO OF ROTOR EXIT TO INLET RADII (MERIDIONAL LINE)

MAP RANGE (ARRAY VALUES MUST BE IN ASCENDING ORDER)

NR           NO OF R VALUES TO BE CALCULATED
AR           ARRAY OF R VALUES(1=STALL,2=MIN-LOSS)
NSPDS        NO OF SPEED LINES
APCNC        ARRAY OF SPEEDS (DECIMAL PERCENT)
NSTP1        NO OF IGV SETTINGS
ASTP1        ARRAY OF IGV ANGLES(-1Ø TO 4Ø DEG)
NROT1        NO OF ROTOR PITCH SETTINGS
AROT1        ARRAY OF ROTOR PITCH ANGLES( -5 TO 5 DEG)


 NAMELIST       INPUT
 ITYPE =           1,
 PQPD  =     1.655Ø,    EFFD  =     Ø.834Ø,
 W1D   =   223.8ØØØ,    PSID  =     Ø.8226,
 WQA1D =    41.Ø7ØØ,    XMZ2D =     Ø.45ØØ,
 SMD   =    14.1ØØØ,    STP1D =     Ø.    ,
 A3QA2 =     Ø.96ØØ,    RRAT  =     Ø.5ØØØ,
 ROQI  =     1.ØØØØ,
 NR    =          11
 AR(I)    =
     1       1.ØØØØ,       1.2ØØØ,       1.4ØØØ,       1.6ØØØ,
     5       1.8ØØØ,       2.ØØØØ,       2.2ØØØ,       2.4ØØØ,
     9       2.6ØØØ,       2.8ØØØ,       3.ØØØØ,
```

```
 NSPDS =          6
 APCNC(I) =
     1       Ø.5ØØØ,        Ø.7ØØØ,        Ø.8ØØØ,        Ø.9ØØØ,
     5       1.ØØØØ,        1.1ØØØ,
 NSTP1 =          3
 ASTP1(I) =
     1       Ø.     ,       2Ø.ØØØØ,       4Ø.ØØØØ,
 NROT1 =          Ø
 AROT1(I) =
     1       Ø.     ,
 END NAMELIST      INPUT
ENTER CHANGES TO NAMELIST INPUT
=$INPUT$

 NAMELIST      INPUT
 ITYPE =         1,
 PQPD  =    1.655Ø,    EFFD  =     Ø.834Ø,
 W1D   =  223.8ØØØ,    PSID  =     Ø.8226,
 WQA1D =   41.Ø7ØØ,    XMZ2D =     Ø.45ØØ,
 SMD   =   14.1ØØØ,    STP1D =     Ø.     ,
 A3QA2 =    Ø.96ØØ,    RRAT  =     Ø.5ØØØ,
 ROQI  =    1.ØØØØ,
 NR    =        11
 AR(I)    =
     1       1.ØØØØ,        1.2ØØØ,        1.4ØØØ,        1.6ØØØ,
     5       1.8ØØØ,        2.ØØØØ,        2.2ØØØ,        2.4ØØØ,
     9       2.6ØØØ,        2.8ØØØ,        3.ØØØØ,
 NSPDS =          6
 APCNC(I) =
     1       Ø.5ØØØ,        Ø.7ØØØ,        Ø.8ØØØ,        Ø.9ØØØ,
     5       1.ØØØØ,        1.1ØØØ,
 NSTP1 =          3
 ASTP1(I) =
     1       Ø.     ,       2Ø.ØØØØ,       4Ø.ØØØØ,
 NROT1 =          Ø
 AROT1(I) =
     1       Ø.     ,
 END NAMELIST      INPUT
OUTPUT ON IFC=3Ø,31,32

PROGRAM COMPLETE  &
```

1001		P-FAN FLOW VS. R, SPEED, AND ANGL						
STP1	3	0.0	20.000	40.000				
SPED	6	0.500	0.700	0.800	0.900	1.000	1.100	
R	11	1.000	1.200	1.400	1.600	1.800	2.000	2.200
R	11	2.400	2.600	2.800	3.000			
FLOW	11	93.3197	100.9660	108.2719	115.1715	121.6018	127.5036	132.6690
FLOW	11	136.8715	138.6807	138.6807	138.6807			
FLOW	11	140.0116	147.5998	154.5570	160.[illegible]	166.5290	171.3347	174.8529
FLOW	11	176.5392	176.7129	176.7129	176.7129			
FLOW	11	164.2152	170.6422	176.8666	182.2923	186.8874	190.7862	193.3546
FLOW	11	194.0171	194.0171	194.0171	194.0171			
FLOW	11	187.6732	192.8620	197.5644	201.7174	205.3210	208.3386	210.3036
FLOW	11	210.7646	210.7646	210.7646	210.7646			
FLOW	11	209.7717	213.2176	216.5546	219.1763	221.6648	223.8120	225.3357
FLOW	11	225.9450	225.9450	225.9450	225.9450			
FLOW	11	227.4914	229.7037	231.8723	233.7958	235.5346	237.0852	238.2061
FLOW	11	238.9715	239.1324	239.1324	239.1324			
SPED	6	0.500	0.700	0.800	0.900	1.000	1.100	
R	11	1.000	1.200	1.400	1.600	1.800	2.000	2.200
R	11	2.400	2.600	2.800	3.000			
FLOW	11	79.0908	85.6275	91.9127	97.6971	103.5341	108.7800	113.5039
FLOW	11	117.5650	120.9125	121.8726	121.8726			
FLOW	11	117.5362	124.6625	131.2496	137.2843	142.7091	147.4722	151.2191
FLOW	11	153.5704	154.4652	154.4761	154.4761			
FLOW	11	137.4297	144.2305	150.4574	156.0514	160.9605	165.1433	168.1275
FLOW	11	169.4122	169.4611	169.4611	169.4611			
FLOW	11	157.4562	163.5344	169.0202	173.8606	178.0440	181.5134	183.7331
FLOW	11	184.2108	184.2108	184.2108	184.2108			
FLOW	11	176.8737	181.9057	186.4038	190.3422	193.6985	196.4565	198.1221
FLOW	11	198.3605	198.3605	198.3605	198.3605			
FLOW	11	195.7194	199.5363	202.5677	205.4037	207.8354	209.8586	211.1310
FLOW	11	211.3733	211.3733	211.3733	211.3733			
SPED	6	0.500	0.700	0.800	0.900	1.000	1.100	
R	11	1.000	1.200	1.400	1.600	1.800	2.000	2.200
R	11	2.400	2.600	2.800	3.000			
FLOW	11	67.3477	72.8335	78.1246	83.1854	87.9807	92.4795	96.6033
FLOW	11	100.2709	103.4467	105.4111	105.4111			
FLOW	11	98.8927	105.0914	110.8983	116.2550	121.1199	125.4542	129.0222
FLOW	11	131.5802	133.0789	133.4896	133.4896			
FLOW	11	115.1530	121.2962	126.9509	132.0662	136.6125	140.5457	143.5455
FLOW	11	145.2662	145.6835	145.6835	145.6835			
FLOW	11	131.2371	137.0771	142.3642	147.0994	151.1319	154.5567	156.9238
FLOW	11	157.7993	157.7993	157.7993	157.7993			
FLOW	11	147.0756	152.3177	156.5920	161.0715	164.5387	167.3803	169.1323
FLOW	11	169.4217	169.4217	169.4217	169.4217			
FLOW	11	162.3147	166.7025	170.1357	173.8036	176.6320	178.9214	180.1747
FLOW	11	180.2639	180.2639	180.2639	180.2639			
EOT								

1002 P-FAN EFF VS. R, SPEED, AND ANGL

STP1	3	0.0	20.000	40.000				
SPED	6	0.500	0.700	0.800	0.900	1.000	1.100	
R	11	1.000	1.200	1.100	1.600	1.800	2.000	2.200
R	11	2.400	2.600	2.900	3.000			
EFF	11	0.7794	0.8141	0.8319	0.8265	0.7083	0.7012	0.5379
EFF	11	0.2419	0.0006	0.0006	0.0006			
EFF	11	0.8230	0.3441	0.8544	0.8511	0.8302	0.7958	0.7100
EFF	11	0.5902	0.4273	0.2070	0.0023			
EFF	11	0.8365	0.8515	0.8592	0.8580	0.8460	0.8205	0.7786
EFF	11	0.7178	0.6502	0.5600	0.4083			
EFF	11	0.8418	0.8515	0.8570	0.8577	0.8529	0.8416	0.8231
EFF	11	0.7976	0.7723	0.7410	0.7025			
EFF	11	0.8300	0.8350	0.8381	0.8390	0.8377	0.8340	0.8277
EFF	11	0.8186	0.8101	0.8014	0.7913			
EFF	11	0.7960	0.7986	0.8004	0.8013	0.8013	0.8003	0.7984
EFF	11	0.7955	0.7915	0.7692	0.7808			
SPED	6	0.500	0.700	0.800	0.900	1.000	1.100	
R	11	1.000	1.200	1.400	1.600	1.800	2.000	2.200
R	11	2.400	2.600	2.800	3.000			
EFF	11	0.7633	0.8122	0.8502	0.8729	0.8735	0.8102	0.7535
EFF	11	0.5741	0.2127	0.0149	0.0149			
EFF	11	0.7997	0.8356	0.8634	0.8802	0.8822	0.8634	0.8157
EFF	11	0.7265	0.5741	0.3956	0.1160			
EFF	11	0.8106	0.8405	0.8637	0.8782	0.8814	0.8694	0.8380
EFF	11	0.7809	0.7177	0.6332	0.5066			
EFF	11	0.8149	0.8383	0.8565	0.8682	0.8719	0.8655	0.8470
EFF	11	0.8190	0.7904	0.7506	0.6955			
EFF	11	0.8105	0.8275	0.8408	0.8497	0.8535	0.8511	0.8419
EFF	11	0.8299	0.8160	0.8017	0.7802			
EFF	11	0.7963	0.8067	0.8148	0.8205	0.8234	0.8231	0.8196
EFF	11	0.8148	0.8116	0.8070	0.8007			
SPED	6	0.500	0.700	0.800	0.900	1.000	1.100	
R	11	1.000	1.200	1.400	1.600	1.800	2.000	2.200
R	11	2.400	2.600	2.800	3.000			
EFF	11	0.7217	0.7736	0.8179	0.8511	0.8681	0.8595	0.8098
EFF	11	0.6874	0.4155	0.0126	0.0126			
EFF	11	0.7491	0.7901	0.8249	0.8510	0.8647	0.8605	0.8305
EFF	11	0.7626	0.6316	0.4393	0.2160			
EFF	11	0.7554	0.7910	0.8209	0.8433	0.8553	0.8528	0.8308
EFF	11	0.7826	0.7454	0.6522	0.5511			
EFF	11	0.7555	0.7857	0.8110	0.8299	0.8402	0.8390	0.8237
EFF	11	0.7924	0.7709	0.7373	0.6850			
EFF	11	0.7492	0.7736	0.7939	0.8090	0.8173	0.8170	0.8071
EFF	11	0.7948	0.7839	0.7666	0.7409			
EFF	11	0.7350	0.7534	0.7685	0.7795	0.7856	0.7836	0.7796
EFF	11	0.7754	0.7707	0.7628	0.7503			
EOT								

ORIGINAL PAGE IS
OF POOR QUALITY

1003	P-FAN PR VS. R, SPEED, AND ANGL						
STPI 3	0.0	20.000	40.000				
SPED 6	0.500	0.700	0.800	0.900	1.000	1.100	
R 11	1.000	1.200	1.400	1.600	1.800	2.000	2.200
R 11	2.400	2.600	2.800	3.000			
PR 11	1.1567	1.1486	1.1364	1.1201	1.0998	1.0758	1.0462
PR 11	1.0175	1.0000	1.0000	1.0000			
PR 11	1.3237	1.3070	1.2851	1.2587	1.2275	1.1980	1.1526
PR 11	1.1097	1.0673	1.0269	1.0003			
PR 11	1.4397	1.4197	1.3951	1.3661	1.3329	1.2958	1.2551
PR 11	1.2119	1.1714	1.1304	1.0893			
PR 11	1.5894	1.5645	1.5441	1.5162	1.4850	1.4507	1.4136
PR 11	1.3745	1.3380	1.3003	1.2625			
PR 11	1.7698	1.7510	1.7301	1.7070	1.6820	1.6550	1.6262
PR 11	1.5958	1.5667	1.5383	1.5097			
PR 11	1.9818	1.9664	1.9497	1.9318	1.9127	1.8924	1.8709
PR 11	1.8485	1.8251	1.8041	1.7832			
SPED 6	0.500	0.700	0.800	0.900	1.000	1.100	
R 11	1.000	1.200	1.400	1.600	1.800	2.000	2.200
R 11	2.400	2.600	2.800	3.000			
PR 11	1.1487	1.1430	1.1336	1.1207	1.1045	1.0851	1.0627
PR 11	1.0378	1.0104	1.0006	1.0006			
PR 11	1.3000	1.2864	1.2680	1.2451	1.2178	1.1866	1.1520
PR 11	1.1148	1.0755	1.0436	1.0095			
PR 11	1.3996	1.3817	1.3588	1.3313	1.2994	1.2634	1.2245
PR 11	1.1836	1.1467	1.1105	1.0736			
PR 11	1.5162	1.4944	1.4681	1.4374	1.4026	1.3642	1.3234
PR 11	1.2833	1.2462	1.2084	1.1700			
PR 11	1.6540	1.6208	1.6017	1.5700	1.5350	1.4968	1.4570
PR 11	1.4192	1.3824	1.3470	1.3101			
PR 11	1.8091	1.7849	1.7580	1.7256	1.6969	1.6631	1.6284
PR 11	1.5955	1.5650	1.5342	1.5029			
SPED 6	0.500	0.700	0.800	0.900	1.000	1.100	
R 11	1.000	1.200	1.400	1.600	1.800	2.000	2.200
R 11	2.400	2.600	2.800	3.000			
PR 11	1.1360	1.1310	1.1230	1.1121	1.0982	1.0816	1.0626
PR 11	1.0414	1.0182	1.0004	1.0004			
PR 11	1.2837	1.2577	1.2413	1.2208	1.1965	1.1687	1.1381
PR 11	1.1059	1.0721	1.0399	1.0150			
PR 11	1.3528	1.3363	1.3152	1.2897	1.2503	1.2273	1.1920
PR 11	1.1558	1.1220	1.0938	1.0647			
PR 11	1.4470	1.4258	1.4000	1.3693	1.3359	1.2986	1.2596
PR 11	1.2214	1.1905	1.1588	1.1264			
PR 11	1.5504	1.5219	1.4951	1.4613	1.4241	1.3839	1.3431
PR 11	1.3074	1.2745	1.2409	1.2066			
PR 11	1.6604	1.6315	1.5991	1.5633	1.5248	1.4838	1.4433
PR 11	1.4096	1.3767	1.3432	1.3091			
EOT							

```
*************PARAMETRIC FLOW MODULATING FAN*************

                    *M*O*D*F*A*N*

AXIAL OR CENT COMPRESSOR? 1=CENT;Ø OR CR=AXIAL
=1

DESCRIPTION OF INPUT VARIABLES IN MODFAN PROGRAM
(NAMELIST INPUT)

ITYPE=1       VIGV
ITYPE=2       VPF(NO IGV )

DESIGN POINT VALUES OF:

PQPD         PRESSURE RATIO(TOTAL-TO-TOTAL)
EFFD         ADIABATIC EFFICIENCY(TOTAL-TO TOTAL)
W1D          INLET CORRECTED FLOW
PSID         ROTOR EXIT MERIDIONAL LOADING(2GJ*DH/U2**2)
WQA1D        INLET CORRECTED FLOW PER UNIT AREA
XMZ2D        MERIDIONAL MACH NO AT ROTOR EXIT
SMD          CONSTANT SPEED STALL MARGIN(PERCENT)
STP1D        IGV METAL ANGLE

GEOMETRY SPECIFICATIONS

A3QA2        STATOR INLET TO ROTOR EXIT AREA RATIO
RRAT         INLET HUB TO TIP RADIUS RATIO
ROQI         RATIO OF ROTOR EXIT TO INLET RADII (MERIDIONAL LINE)

MAP RANGE (ARRAY VALUES MUST BE IN ASCENDING ORDER)

NR           NO OF R VALUES TO BE CALCULATED
AR           ARRAY OF R VALUES(1=STALL,2=MIN-LOSS)
NSPDS        NO OF SPEED LINES
APCNC        ARRAY OF SPEEDS (DECIMAL PERCENT)
NSTP1        NO OF IGV SETTINGS
ASTP1        ARRAY OF IGV ANGLES(-1Ø TO 4Ø DEG)
NROT1        NO OF ROTOR PITCH SETTINGS
AROT1        ARRAY OF ROTOR PITCH ANGLES( -5 TO 5 DEG)

 NAMELIST       INPUT
 ITYPE =          1,
 PQPD  =     4.3ØØØ,     EFFD  =     Ø.76ØØ,
 W1D   =     5.5ØØØ,     PSID  =     1.816Ø,
 WQA1D =    35.31ØØ,     XMZ2D =     Ø.295Ø,
 SMD   =    1Ø.ØØØØ,     STP1D =     Ø.    ,
 A3QA2 =     1.Ø5ØØ,     RRAT  =     Ø.275Ø,
 ROQI  =     2.Ø3ØØ,
 NR    =         11
 AR(I)     =
     1       1.ØØØØ,         1.2ØØØ,         1.4ØØØ,         1.6ØØØ,
     5       1.8ØØØ,         2.ØØØØ,         2.2ØØØ,         2.4ØØØ,
     9       2.6ØØØ,         2.8ØØØ,         3.ØØØØ,
```

```
 NSPDS =          6
 APCNC(I) =
     1        Ø.5ØØØ,        Ø.7ØØØ,        Ø.8ØØØ,        Ø.9ØØØ,
     5        1.ØØØØ,        1.1ØØØ,
 NSTP1 =          1
 ASTP1(I) =
     1        Ø.     ,
 NROT1 =          Ø
 AROT1(I) =
     1        Ø.     ,
 END NAMELIST       INPUT
ENTER CHANGES TO NAMELIST INPUT
=$INPUTS

 NAMELIST       INPUT
 ITYPE =          1,
 PQPD  =     4.3ØØØ,    EFFD  =     Ø.76ØØ,
 WID   =     5.5ØØØ,    PSID  =     1.816Ø,
 WQA1D =    35.31ØØ,    XMZ2D =     Ø.295Ø,
 SMD   =    1Ø.ØØØØ,    STP1D =     Ø.     ,
 A3QA2 =     1.Ø5ØØ,    RRAT  =     Ø.275Ø,
 ROQI  =     2.Ø3ØØ,
 NR    =         11
 AR(I)    =
     1        1.ØØØØ,        1.2ØØØ,        1.4ØØØ,        1.6ØØØ,
     5        1.8ØØØ,        2.ØØØØ,        2.2ØØØ,        2.4ØØØ,
     9        2.6ØØØ,        2.8ØØØ,        3.ØØØØ,
 NSPDS =          6
 APCNC(I) =
     1        Ø.5ØØØ,        Ø.7ØØØ,        Ø.8ØØØ,        Ø.9ØØØ,
     5        1.ØØØØ,        1.1ØØØ,
 NSTP1 =          1
 ASTP1(I) =
     1        Ø.     ,
 NROT1 =          Ø
 AROT1(I) =
     1        Ø.     ,
 END NAMELIST       INPUT
OUTPUT ON IFC=3Ø,31,32

PROGRAM COMPLETE   &
```

1001	P-FAN FLOW VS. R, SPEED, AND ANGL						
STP1 1	0.0						
SPED 6	0.500	0.700	0.800	0.900	1.000	1.100	
R 11	1.000	1.200	1.400	1.600	1.800	2.000	2.200
R 11	2.400	2.600	2.800	3.000			
FLOW 11	2.1464	2.2372	2.3270	2.4156	2.5029	2.5888	2.6730
FLOW 11	2.7553	2.8355	2.9135	2.9591			
FLOW 11	3.2070	3.3132	3.4175	3.5198	3.6200	3.7180	3.8127
FLOW 11	3.9032	3.9892	4.0706	4.1469			
FLOW 11	3.7912	3.8982	4.0033	4.1062	4.2069	4.3051	4.3997
FLOW 11	4.4892	4.5732	4.6517	4.7243			
FLOW 11	4.4077	4.5106	4.6116	4.7105	4.8073	4.9017	4.9924
FLOW 11	5.0777	5.1572	5.2308	5.2932			
FLOW 11	5.0481	5.1420	5.2342	5.3246	5.4132	5.4999	5.5831
FLOW 11	5.6611	5.7337	5.8008	5.8620			
FLOW 11	5.6978	5.7771	5.8552	5.9320	6.0075	6.0815	6.1527
FLOW 11	6.2197	6.2824	6.3405	6.3940			
EOT							

1002		P-FAN EFF VS. R, SPEED, AND ANGL						
STP1	1	0.0						
SPED	6	0.500	0.700	0.800	0.900	1.000	1.100	
R	11	1.000	1.200	1.400	1.600	1.800	2.000	2.200
R	11	2.400	2.600	2.800	3.000			
EFF	11	0.8195	0.8210	0.8217	0.8213	0.8199	0.8175	0.8142
EFF	11	0.8098	0.8045	0.7982	0.7909			
EFF	11	0.8259	0.8272	0.8278	0.8278	0.8272	0.8260	0.8242
EFF	11	0.8217	0.8187	0.8150	0.8107			
EFF	11	0.8136	0.8147	0.8152	0.8154	0.8151	0.8143	0.8130
EFF	11	0.8113	0.8092	0.8066	0.8035			
EFF	11	0.7918	0.7926	0.7932	0.7933	0.7932	0.7928	0.7920
EFF	11	0.7909	0.7895	0.7878	0.7858			
EFF	11	0.7590	0.7596	0.7600	0.7602	0.7602	0.7600	0.7596
EFF	11	0.7589	0.7581	0.7571	0.7559			
EFF	11	0.7103	0.7107	0.7110	0.7111	0.7112	0.7111	0.7109
EFF	11	0.7106	0.7101	0.7096	0.7089			
EOT								

ORIGINAL PAGE IS
OF POOR QUALITY

1003		P-FAN PR VS. R, SPEED, AND ANGL						
STP1	1	0.0						
SPED	6	0.500	0.700	0.800	0.900	1.000	1.100	
R	11	1.000	1.200	1.400	1.600	1.800	2.000	2.200
R	11	2.400	2.600	2.800	3.000			
PR	11	1.5766	1.5749	1.5723	1.5690	1.5650	1.5601	1.5544
PR	11	1.5481	1.5410	1.5333	1.5248			
PR	11	2.3420	2.3367	2.3310	2.3281	2.3208	2.3123	2.3025
PR	11	2.2915	2.2734	2.2661	2.2517			
PR	11	2.8961	2.8920	2.8864	2.8793	2.8708	2.8607	2.8493
PR	11	2.8365	2.8224	2.8070	2.7903			
PR	11	3.5714	3.5657	3.5605	3.5528	3.5435	3.5327	3.5204
PR	11	3.5068	3.4918	3.4754	3.4576			
PR	11	4.3386	4.3337	4.3274	4.3197	4.3105	4.3000	4.2880
PR	11	4.2748	4.2602	4.2444	4.2274			
PR	11	5.0864	5.0816	5.0758	5.0688	5.0606	5.0513	5.0410
PR	11	5.0296	5.0171	5.0036	4.9891			
EOT								

7.0 ANALYTICAL BACKGROUND

7.1 Method of Map Generation

The fan geometry is defined implicitly by the design point input, and the user selected option such as VIGV settings etc. The rotor design parameters are first separated from those of the IGV and stator. The rotor is then analyzed separately and the IGV and stator losses added on after the rotor calculation has been completed.

The min-loss line which forms the backbone of the map is assumed to pass through the design point. This sets the optimum incidence angle on the rotor. The flow coefficient (Cz_1/U_1) is assumed to remain constant with speed along the min-loss line for any given value of STP1 or ROT1. The work coefficient ($2g\ J\ DH/U_2^2$) is obtained from the flow coefficient, rotor geometry, and rotor continuity. The rotor loss at min-loss is obtained at the design point. This loss is assumed to be a function of rotor inlet relative Mach number only since at design point the incidence is assumed optimum. A curve of loss vs. rotor inlet relative Mach number is used with a scalar to force the loss through the design point value. For off-design the incidence loss is assumed to vary as ($1-\cos^{\eta} i$) where η is determined from the NASA TASK II data of Ref. 4.

In order to indicate how different IGV positions are calculated, consider the min-loss point on the 100% speed line. Assume an IGV setting of STP1= +20° is required. The rotor exit relative flow angle (BETA2) is assumed to remain constant. The flow coefficient and work coefficient are then calculated from the known value of ALPHA1 and BETA1. A slight shift in the min-loss value of BETA1 and IGV position has been observed in the data and is applied as a correction to BETA1 before the calculation is made.

The rotor continuity iteration to determine the axial valocity ratio across the rotor is the key iteration in the program. The results of this iteration together with the known flow angles sets the work coefficient at min-loss.

To determine the off-backbone characteristics, the angles ALPHA1 and BETA2 are assumed equal to their min-loss values at the selected speed. A value of the work coefficient is then chosen and the rotor continuity iteration carried out. The stator and IGV losses are then added to obtain the stage performance.

7.2 Discussion of Variable Geometry Options for Axial Flow Fans

7.2.1 Variable Inlet Guide Vane (VIGV) Option

The VIGV option can be used to generate a set of off-design performance maps for a user selected design point and set of IGV angles (i.e., STP1). The design point is assumed to be at a zero value of STP1. The VIGV are assumed to be of the type tested in the NASA TASK II program (Ref. 4), i.e., of a flap-type as sketched in Figure 4. Since the IGV leading edge does not move, no IGV incidence loss is included in the stage loss calculation. The inlet flow angle (ALPHA1) is somewhat less than the IGV angle (STP1). As currently set the ratio of ALPHA1 to STP1 is about 0.775, as determined from the data of Ref. 4.

The nature of the flow modulation produced by the VIGV's is illustrated in Figure 4. Let the nominal IGV setting represent the design point. Then at the same speed and rotor incidence angle, the closed position results in a smaller value of inlet axial velocity and, therefore, a smaller flow. A similar line of reasoning leads to the conclusions that a negative IGV setting results in a flow increase.

The above conclusions can be made somewhat clearer and more quantative by referring to the stage characteristic sketch shown in Figure 5. The fan stage characteristic can be expressed in either of the following two ways.

$$\psi = 2 - 2\phi_1 \left(\tan\alpha_1 + C_{z2}/C_{z1} \tan\beta_2 \right) \qquad (1)$$

$$\psi = 2\phi_1 \left(\tan\beta_1 - C_{z2}/C_{z1} \tan\beta_2 \right) \qquad (2)$$

where $\psi = \Delta H / U^2/2g_0J$; $\phi_1 = C_{z1}/U_1$

α_1 = absolute inlet angle
β_1 = relative inlet angle
β_2 = relative exit angle

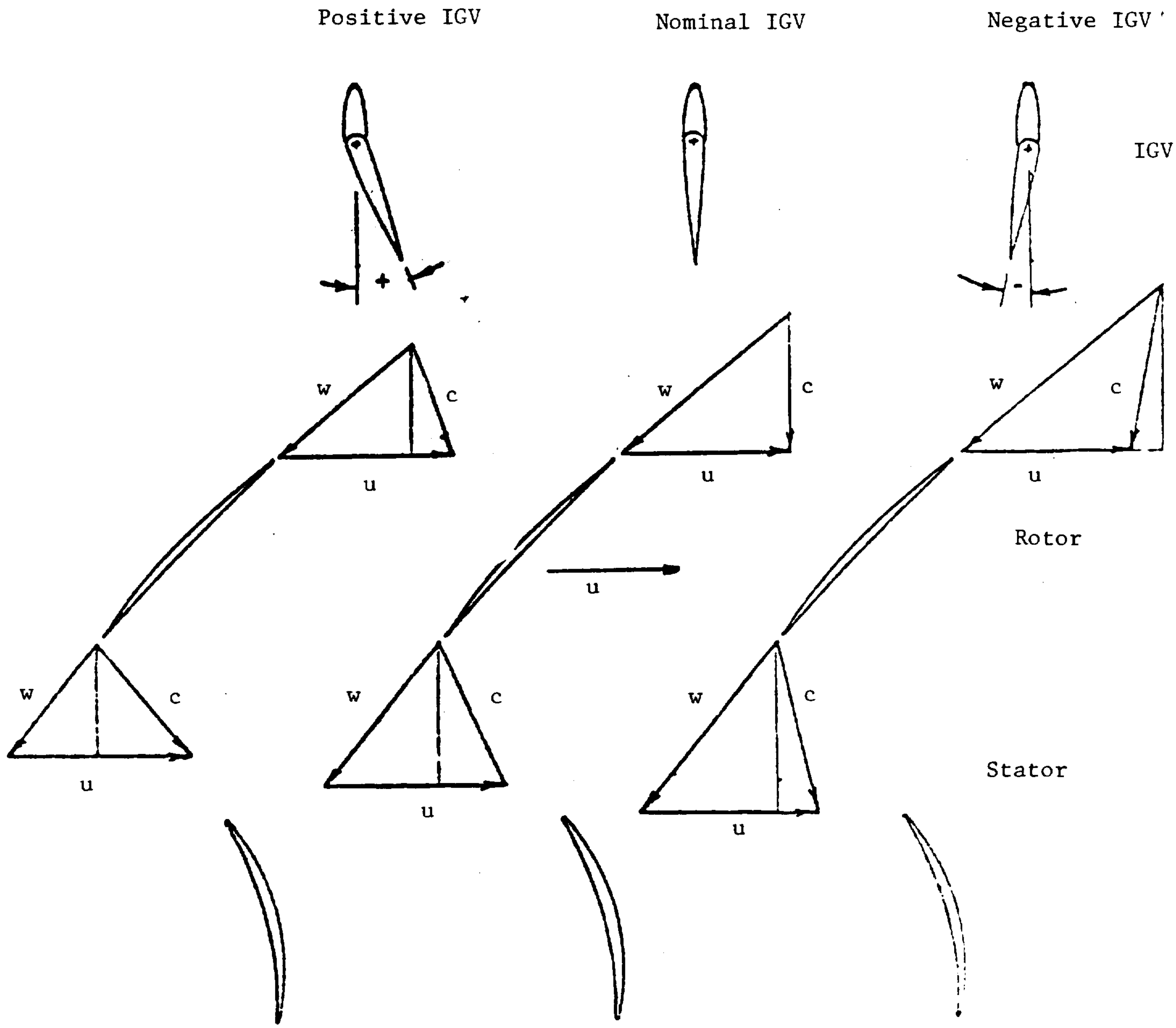

Figure 4. Vector Diagram for Variable Inlet Guide Vanes (VIGV) at Constant Rotor Incidence and Deviation Angle.

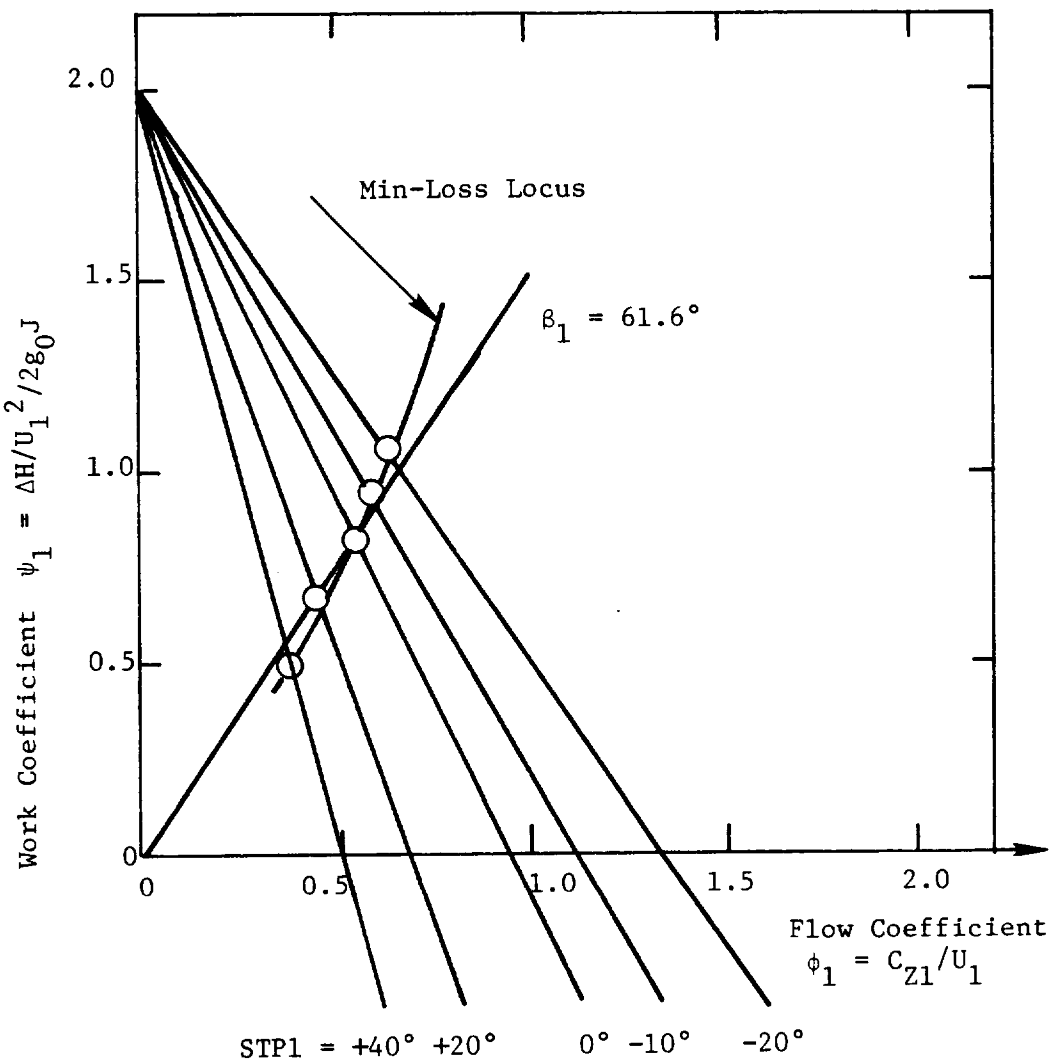

Figure 5. Stage Characteristics for VIGV Axial-Flow Fan.

If the axial velocity ratio (C_{z2}/C_{z1}) and the exit flow angle are assumed to be constant, then equation one is a straight line passing through two (2) when the flow coefficient equals zero. A series of these lines for different values of STP1 (ALPHA1 = 0.775 x STP1) are shown in Figure 5. Also shown in Figure 5 is a line of constant incidence angle passing through the design point (as given by equation 2). The locus of the min-loss point on the 100% speed line,as generated by the programs, has also been indicated in the figure. It can be seen from Figure 5 that the min-loss locus closely follows a line of constant rotor incidence angle. The changing flow coefficient explains the flow modulation observed. Parametric maps generated for the NASA TASK II VIGV Comparison (Ref. 4) are shown in Figures 6 thru 9. One negative angle map was generated from the program in order to show the basic trends. Test data is reported in (Ref. 4) includes three positive IGV positions (0°, 20°, and 40°) and no negative IGV settings.

The test data of Reference 4 was compared with the program results along the min-loss locus. These comparison plots are shown in Figure 10, 11 and 12. As can be seen from the plots, as the IGV are closed, both the flow and the pressure rise decrease. In general, the agreement between the map and the test data is quite good. All of the trends in the data are correctly predicted by the program.

7.2.2 Variable Pitch Rotor (VPF) Option

The VPF option can be used to generate a set of off-design performance maps for a user selected design point and set of rotor pitch angles (i.e., ROT1). As with the VIGV option, the design point is assumed to be at a zero value of ROT1. IGV are assumed to be absent in this option.

The nature of the flow modulation produced by the VPF is illustrated in Figure 13. Let the nominal pitch setting represent the design point. Then at the same speed and zero incidence angle the positive pitch (i.e., rotor closing) has a smaller value of axial velocity than the nominal pitch. This results in less flow as the rotor is closed.

As with VIGV, the same conclusions follow from the stage characteristic. This is shown in Figure 14. Note thate the min-loss locus generated by the program closely follows zero rotor incidence angle. The relative flow angle corresponding to zero incidence is changed by varying the pitch of the rotor. Note that the min-loss locus is nearly horizontal for the VPF while for the VIGV's the locus sloped upward from the origin.

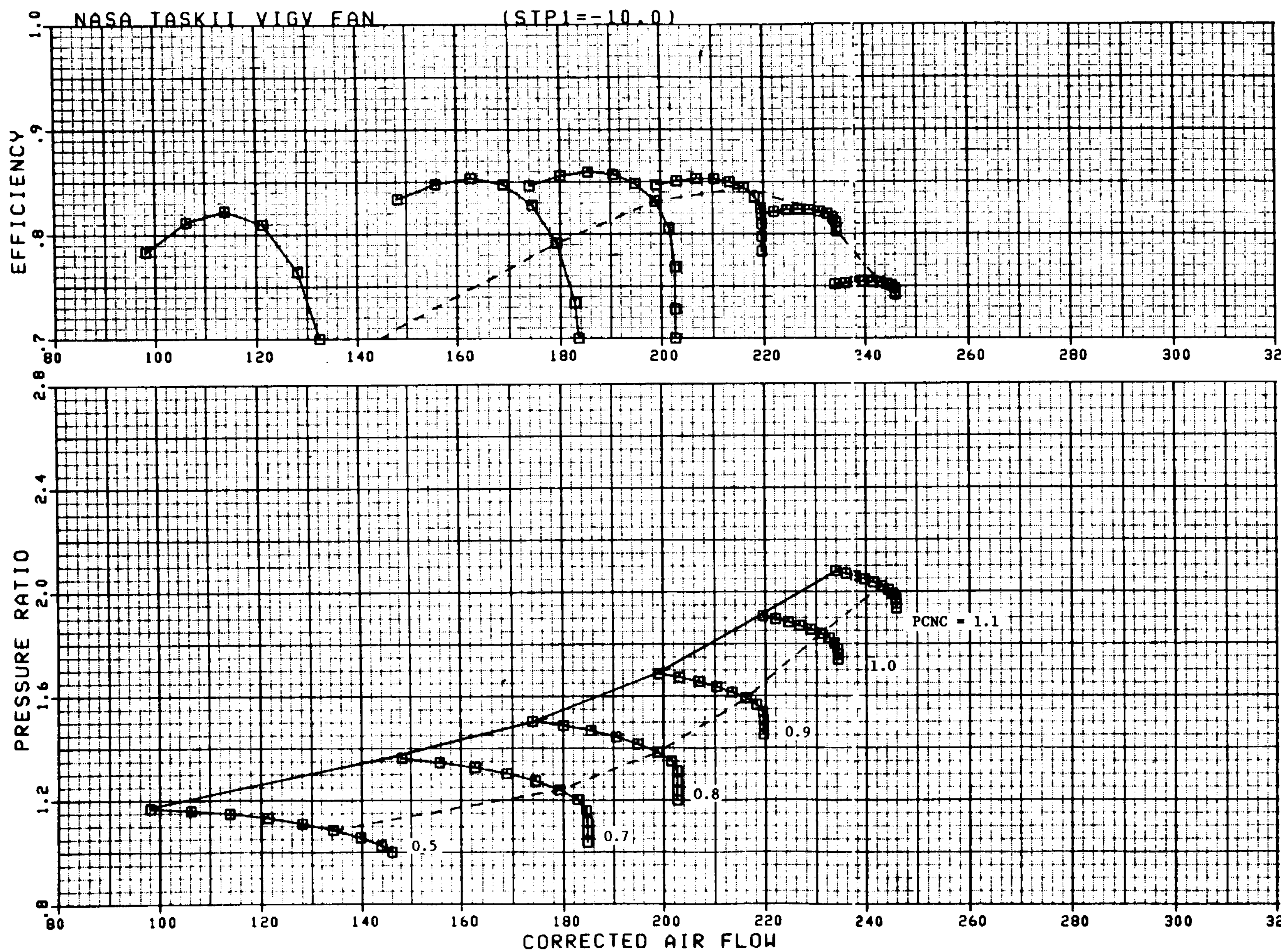

Figure 6. Parametric IVGV Axial Flow Fan (STP1 = -10.0°).

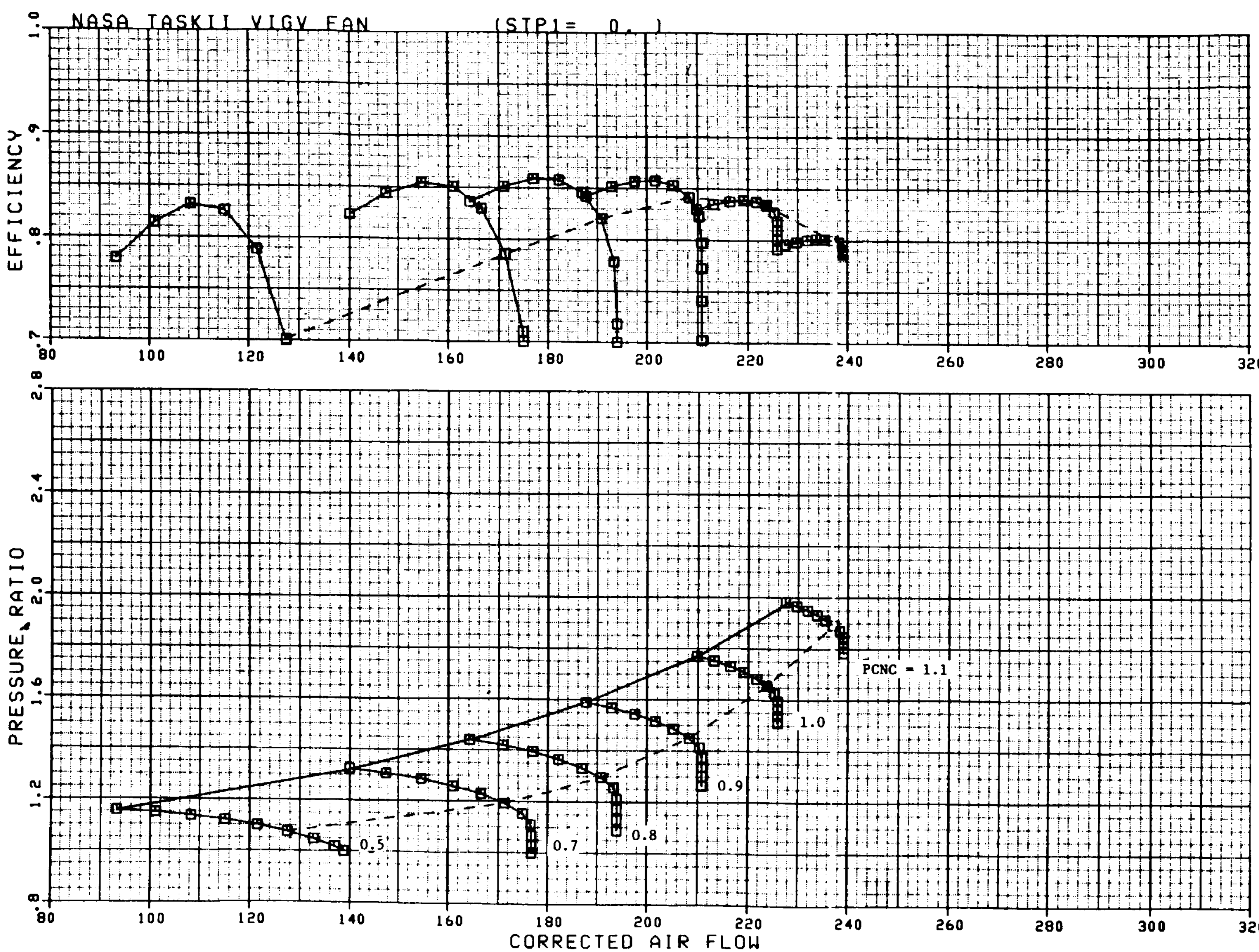

Figure 7. Parametric VIGV Axial Flow Fan (STP1 = 0.0°).

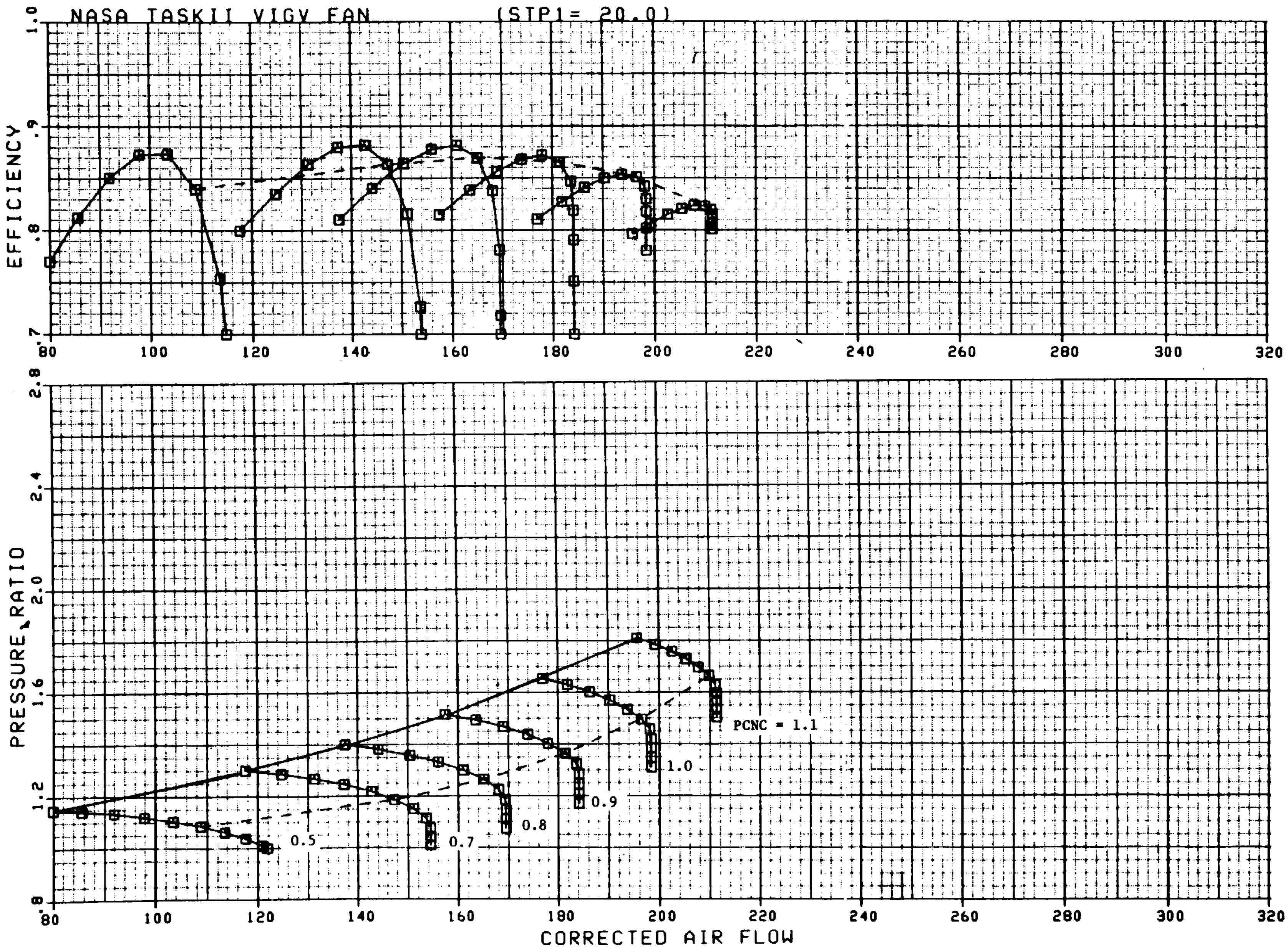

Figure 8. Parametric VIGV Axial Flow Fan (STP1 = +20.0°).

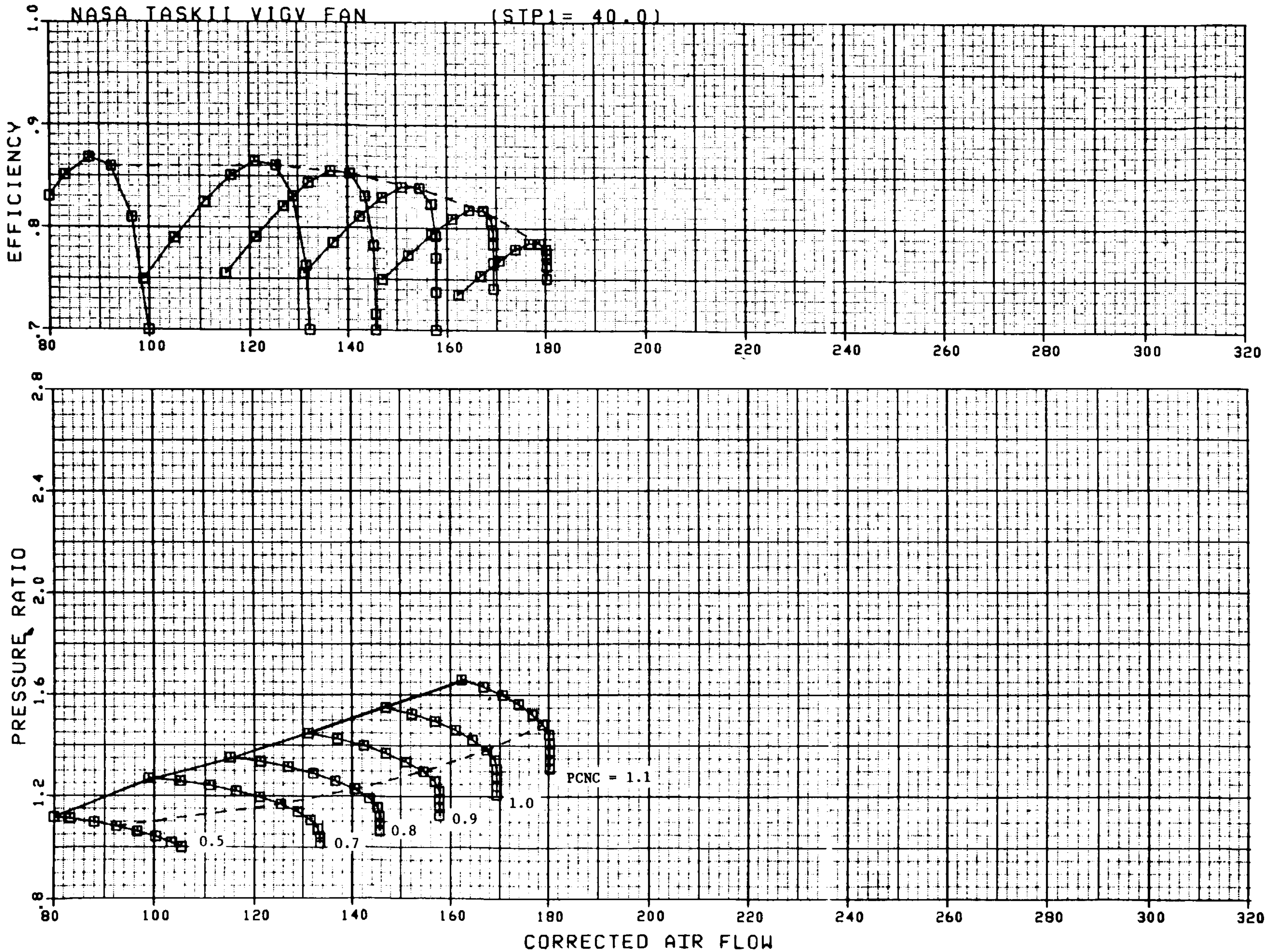

Figure 9. Parametric VIGV Axial Flow Fan (STP1 = +40.0°).

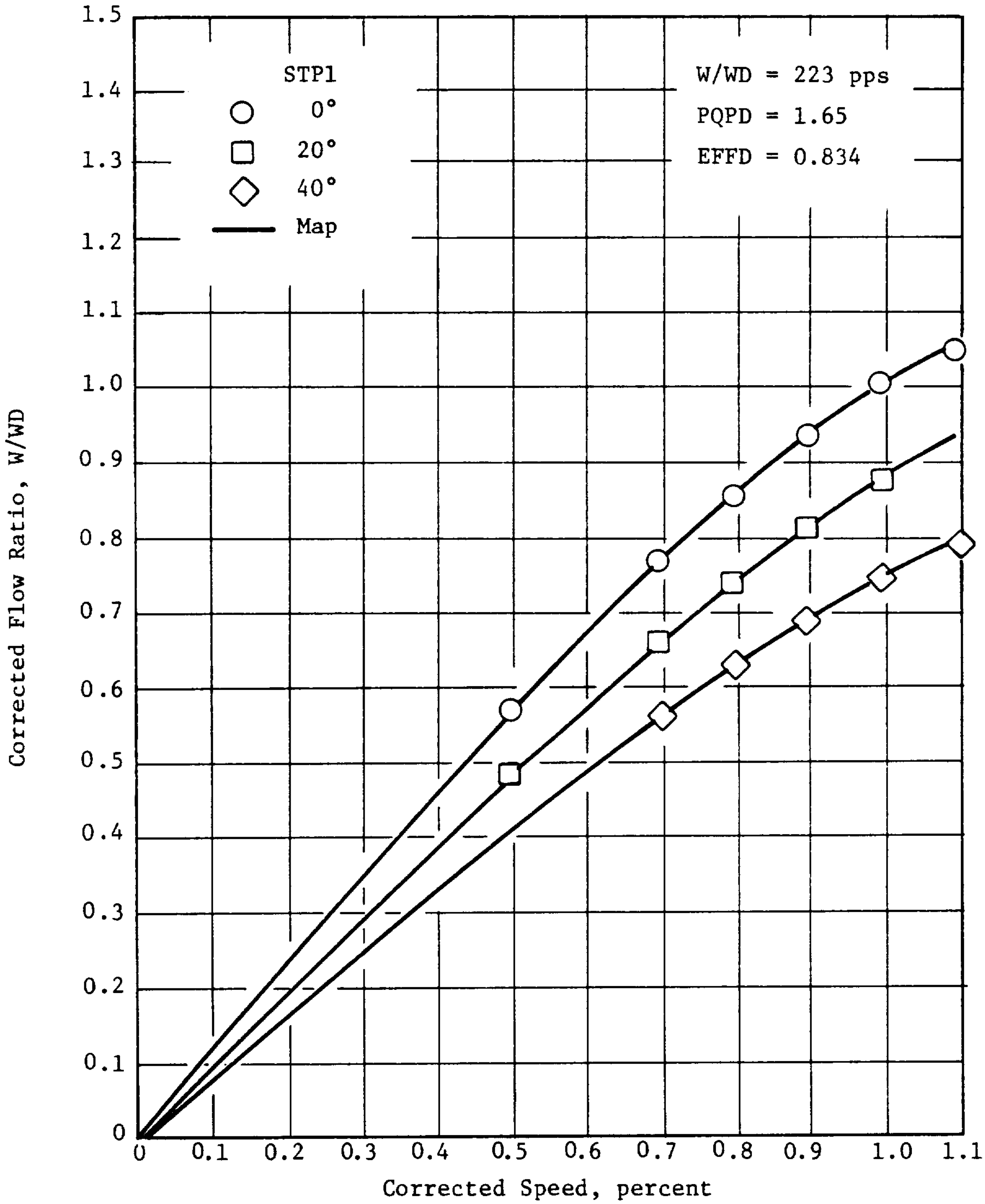

Figure 10. Flow Variation Along Min-Loss Locus (Single Stage VIGV Fan).

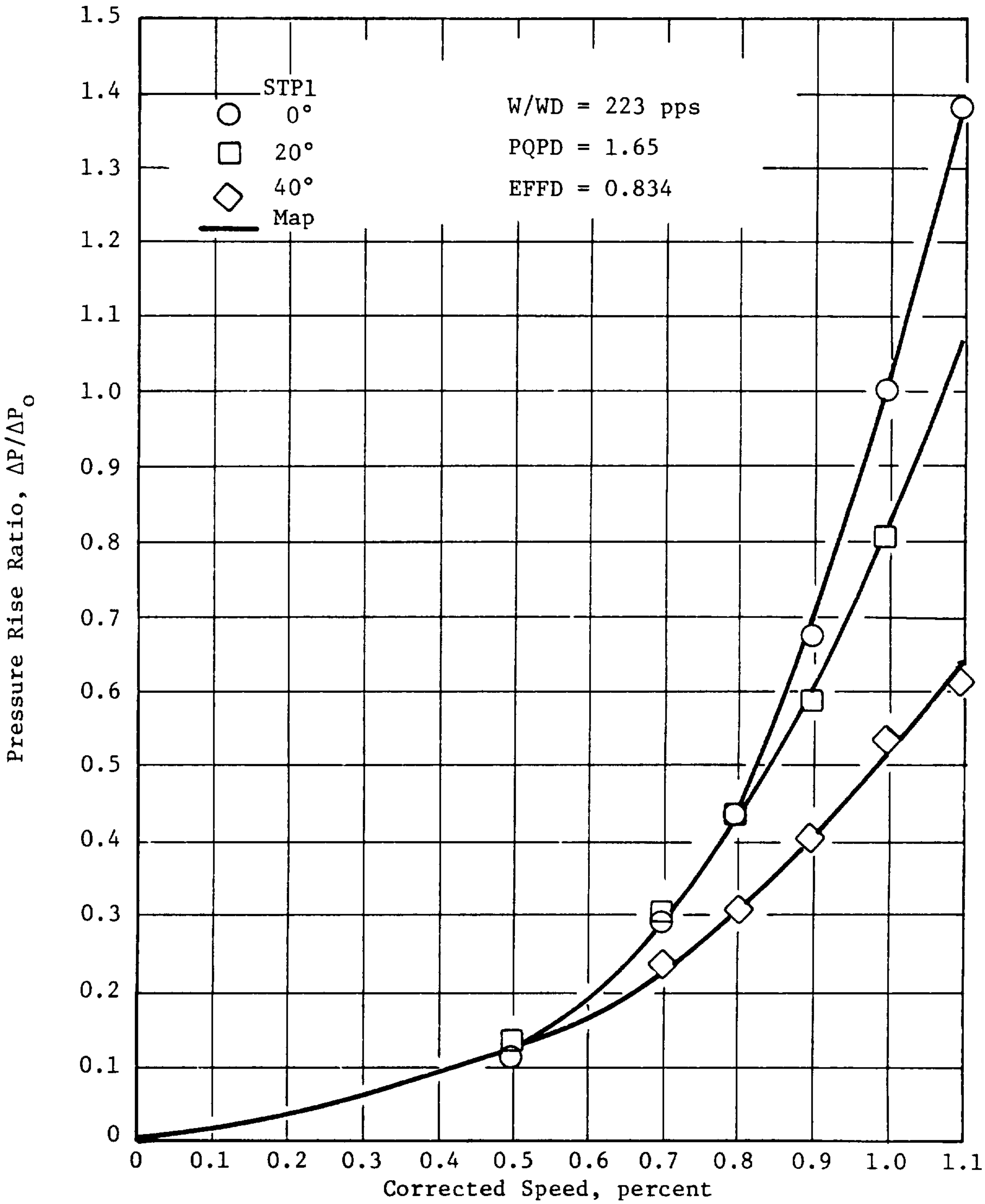

Figure 11. Pressure Rise Variation Along Min-Loss Locus (Single Stage VIGV Fan).

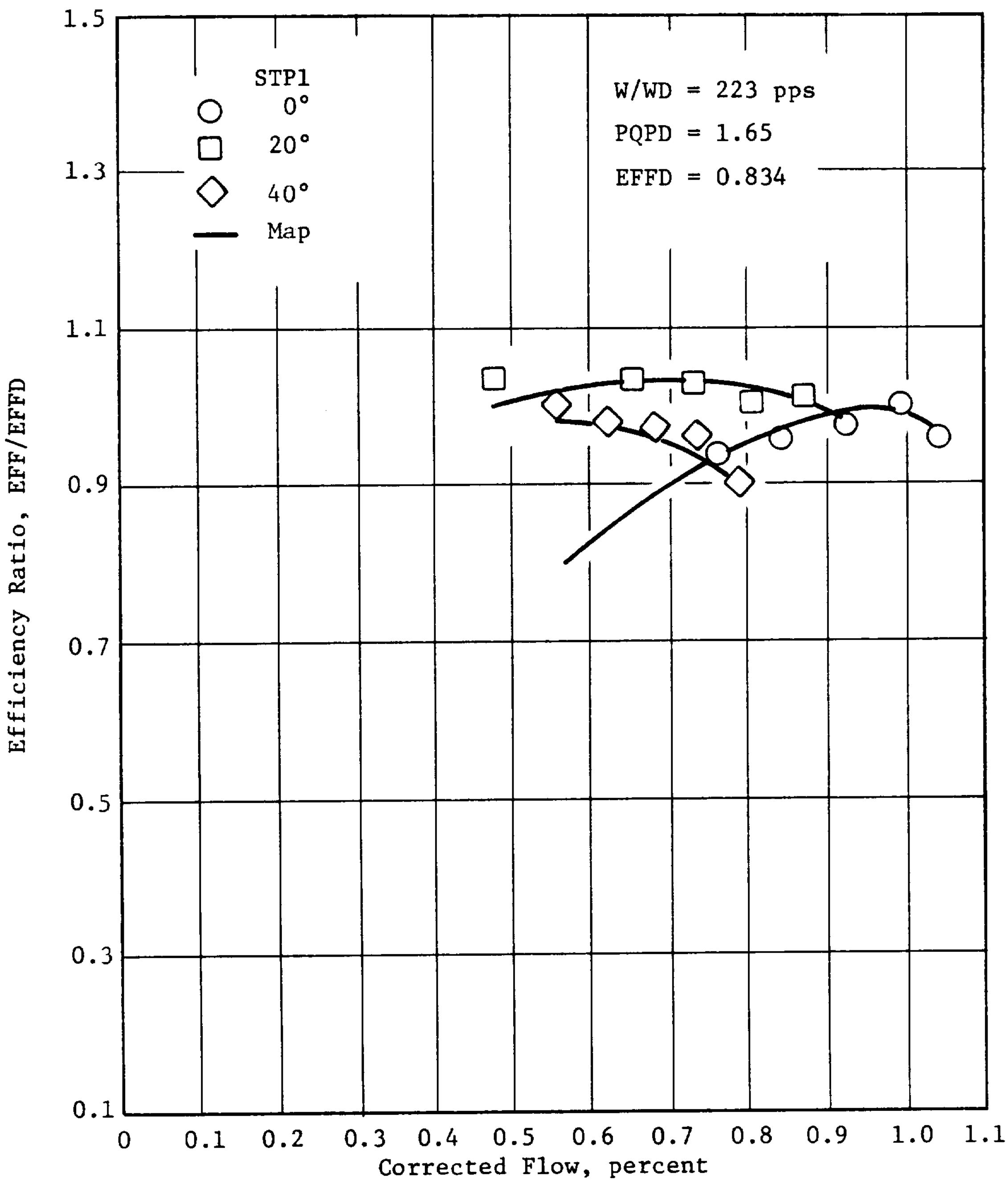

Figure 12. Efficiency Variation Along Min-Loss Locus (Single Stage VIGV Fan).

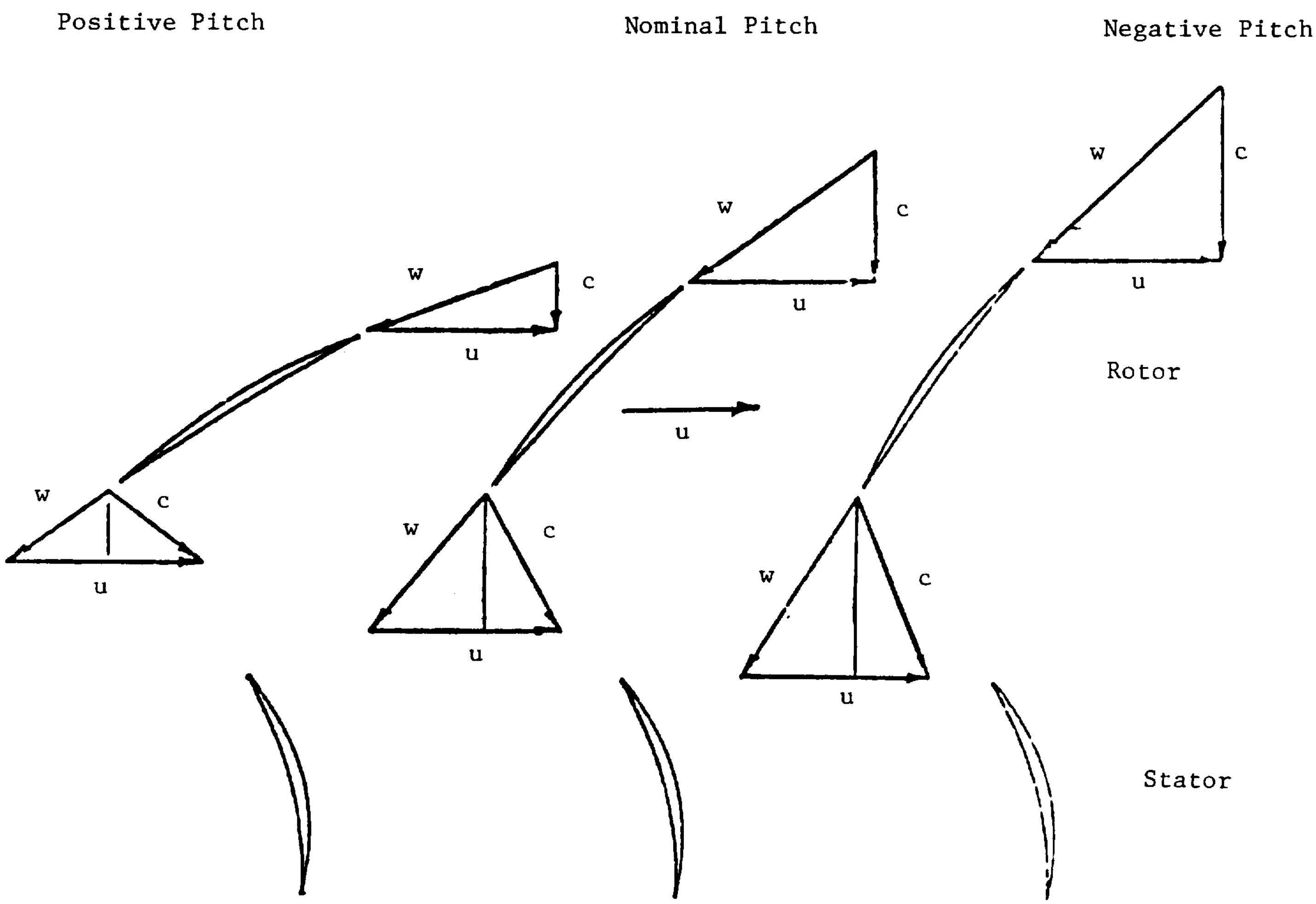

Figure 13. Vector Diagram for Variable Pitch Rotor (VPF).

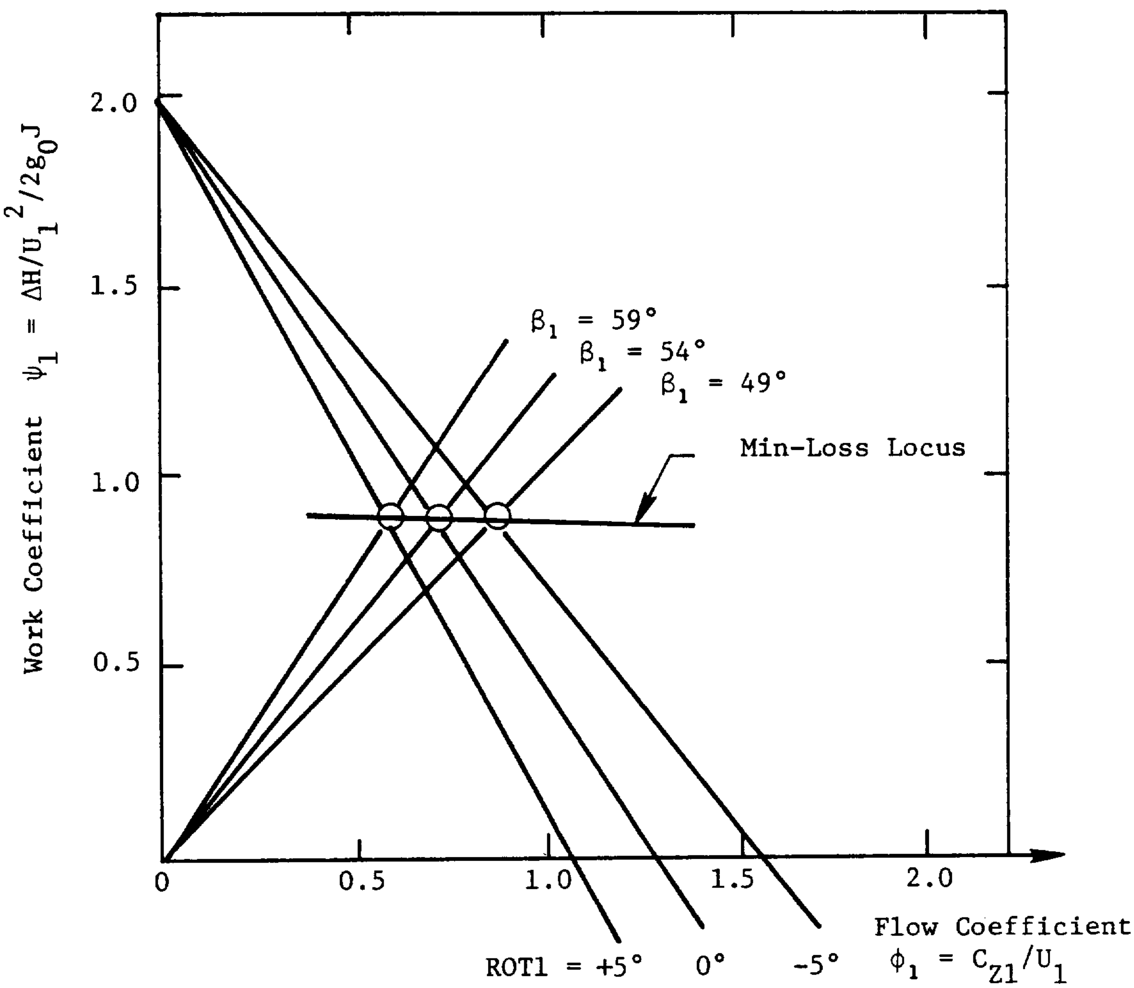

Figure 14. Stage Characteristics for VPF.

7.3 Discussion of Centrifugal Compressor Option

7.3.1 Fixed Geometry Centrifugal Compressors

The centrifugal compressor option can be used to generate a set of off-design performance maps for a user selected design point. The default settings assume a geometry consisting of an impellor followed by a radial diffuser. The inlet swirl angle is assumed to be zero and no provision is made for inlet guide vane loss.

The test data of Reference 5 was compared with the program results for the centrifugal compressor default case along the min-loss locus. These comparison plots are shown in Figure 15, 16, and 17. In general, the agreement between the map and the test data is fairly good. All of the trends in the data are correctly predicted by the program.

7.3.2 Variable Inlet Guide Vanes (VIGV)

Centrifugal compressors frequently have a substantial degree of inlet swirl. This swirl may result from the presence of an upstream axial compressor, or from the presence of inlet guide vanes. In order to account for inlet swirl at the design point, the program has provision for user selection of the design point inlet guide vane position (STP1D). The turning effectiveness of the IGV is assumed to 0.775 (i.e., ANGA1 = 0.775 x STP1). No loss is charged to the IGV.

A variable inlet guide vane option (VIGV) has been provided for the centrifugal compressor just as for the axial flow fan. The most significant difference between the axial and centrifugal VIGV options is that no loss is charged to the inlet guide vanes in the latter case.

The nature of the flow modulation produced by the VIGV's for the centrifugal machine is somewhat different from that for an axial machine. This can be made clear by comparing the stage characteristics for the VIGV centrifugal compressor with those of the axial flow fan which was shown in Figure 5.

The stage characteristic for a centrifugal compressor can be expressed in either of the following two ways;

$$\psi = 2 - 2\phi \left(\frac{R_1}{R_2}\right)^2 \left[\tan\alpha_1 + \frac{\zeta_2}{\zeta_1}\frac{R_2}{R_1} \tan\beta_2 \right] \qquad (3)$$

$$\psi = 2\left(1 - (R_1/R_2)^2\right) + 2\phi_1 \left(\frac{R_1}{R_2}\right)^2 \left[\tan\beta_1 - \frac{\zeta_2}{\zeta_1}\frac{R_2}{R_1} \tan\beta_2 \right] \qquad (4)$$

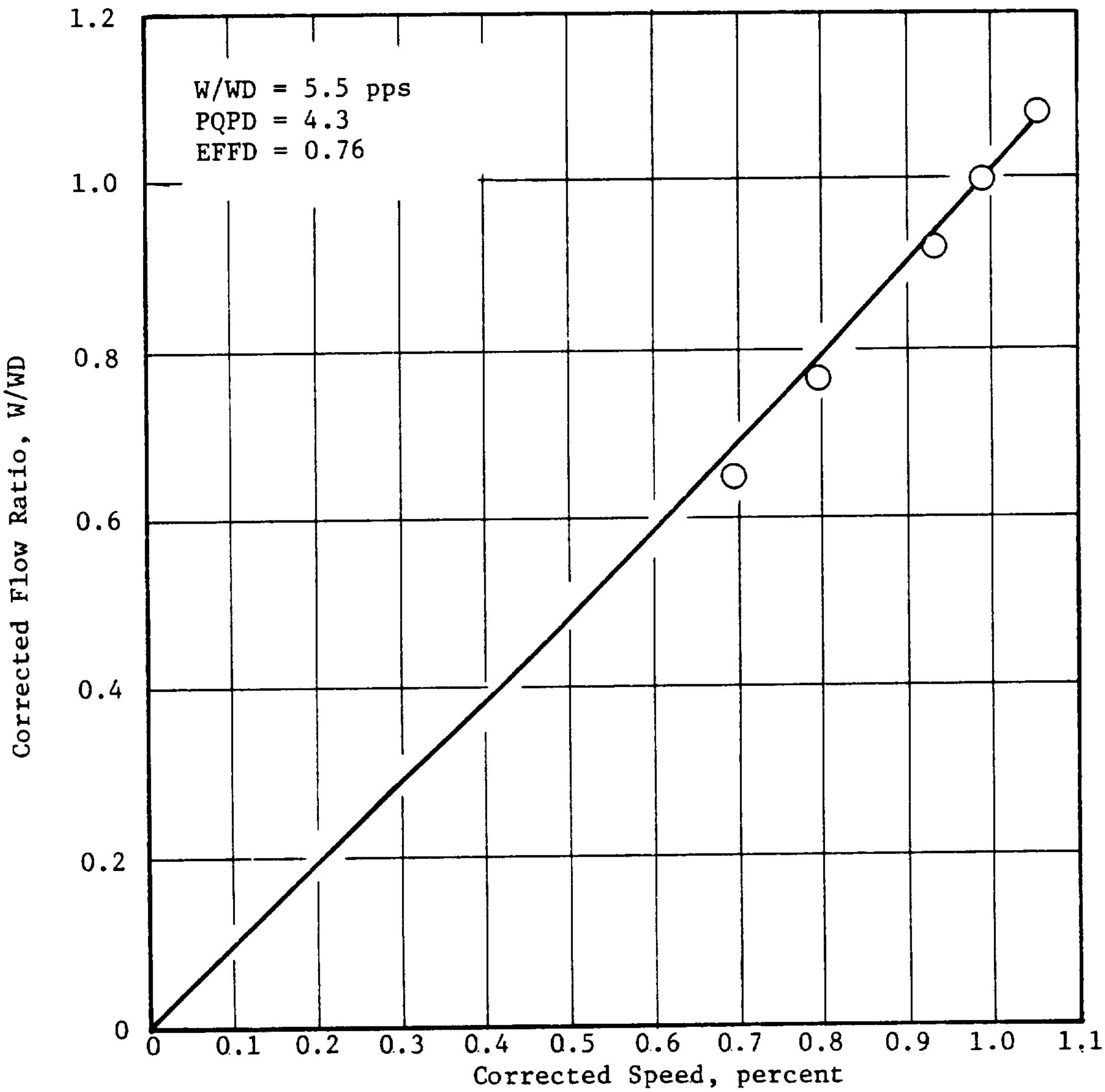

Figure 15. Flow Variation Along Min-Loss Line (Centrifugal Compressor).

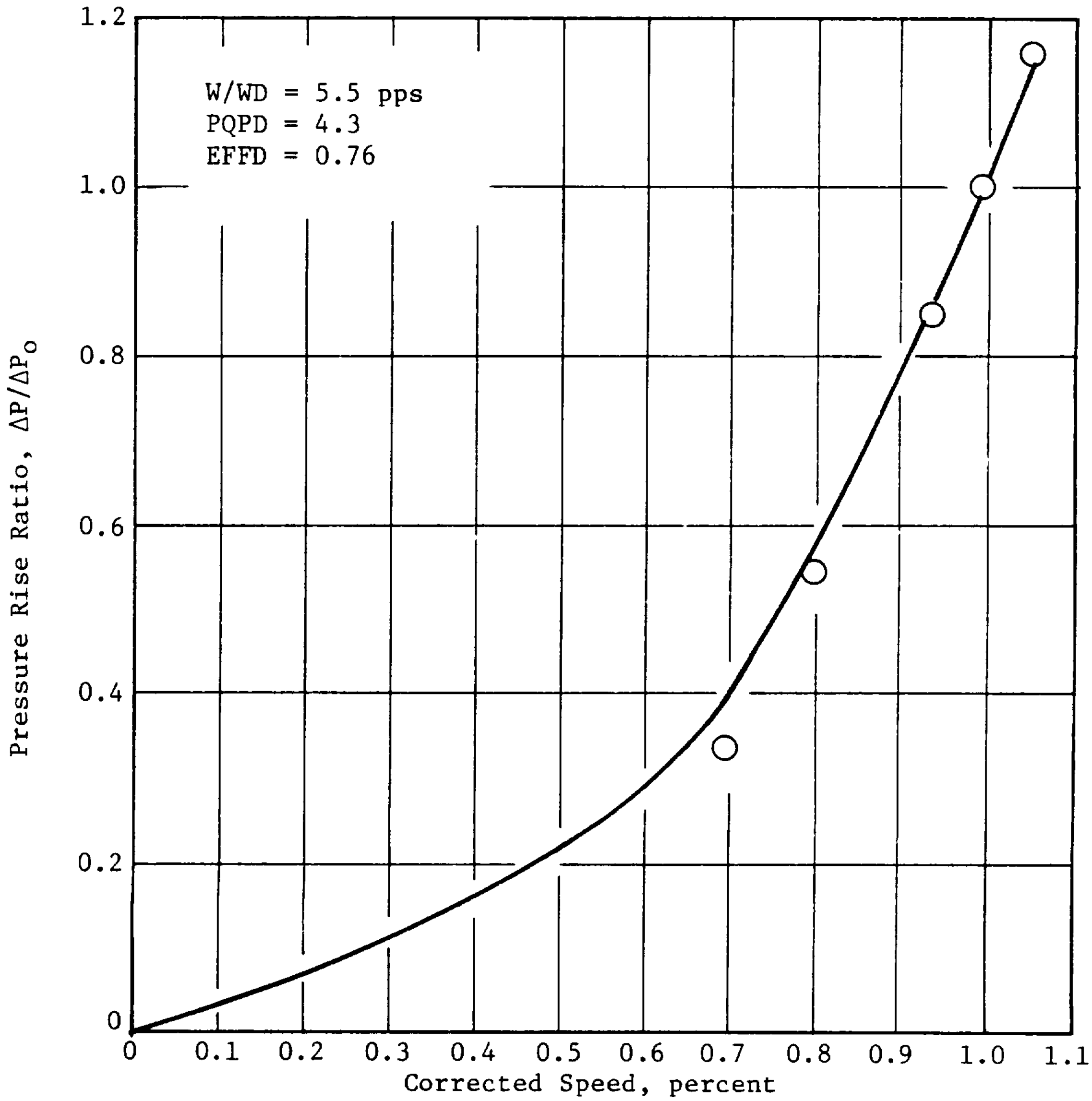

Figure 16. Pressure Rise Variation Along Min-Loss Locus (Centrifugal Compressor).

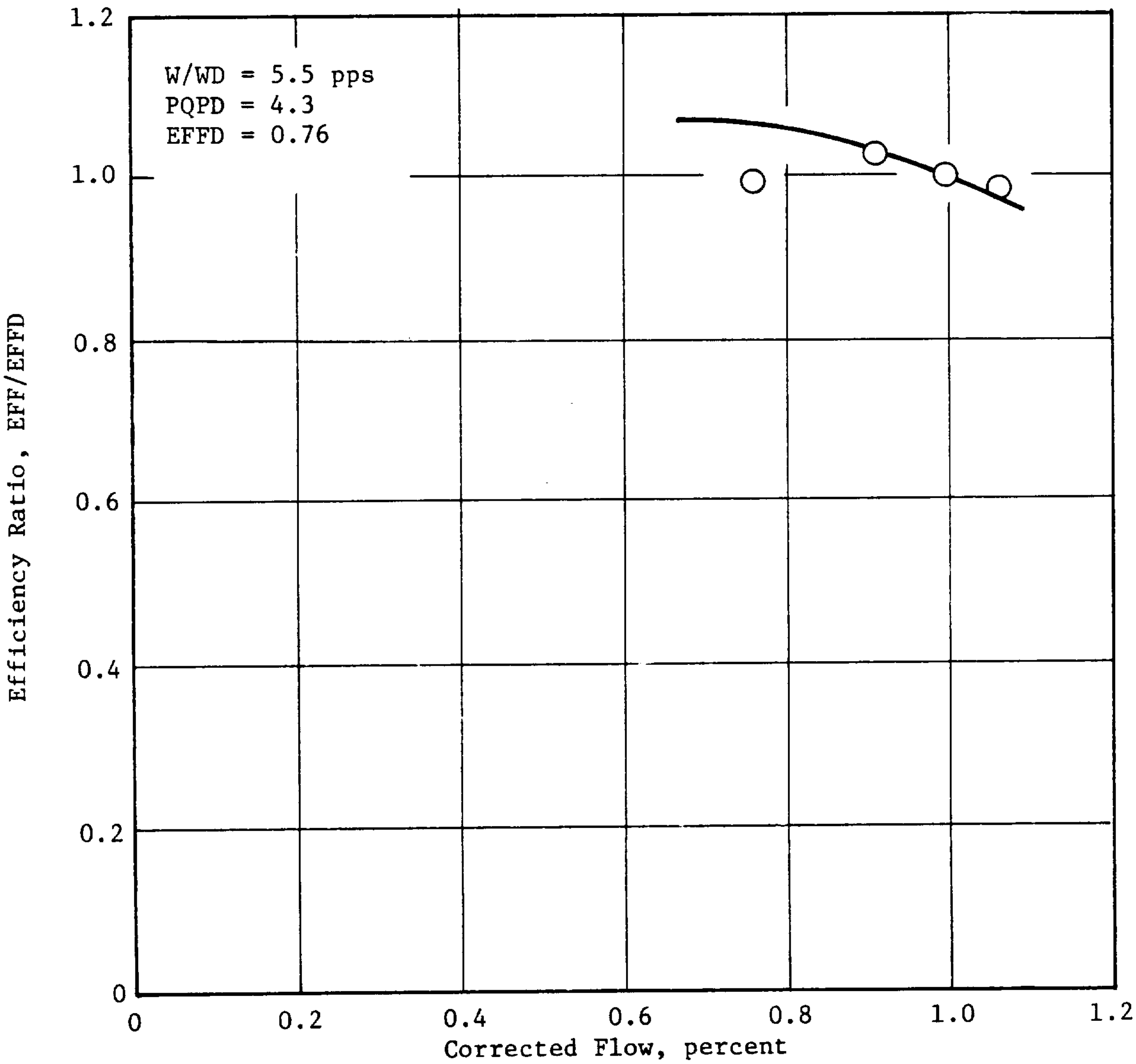

Figure 17. Efficiency Variation Along Min-Loss Locus (Centrifugal Compressor).

Equations three and four reduce to equations one and two if the ratio of the inlet to exit radii is set equal to unity.

If the axial velocity ratio (C_{z2}/C_{z1}) and the exit flow angle are assumed to be constant, then equation three is a straight line passing through two (2) when the flow coefficient equals zero. A series of these lines for different values of STP1 (ALPHA1 = 0.775 x STP1) are shown in Figure 18. Also shown in Figure 18 is a line of constant incidence angle passing through the design point (as given by equation 4). The locus of the min-loss point on the 100% speed line has also been indicated in the figure. It can be seen from Figure 18that the min-loss locus closely follows a line of constant rotor incidence angle. The flow modulation results from the change in flow coefficient along this locus.

Note that the value of the min-loss work coefficient increases as the flow coefficient is reduced. This behavior contrast with that of the VIGV axial flow fan shown in Figure 5 , where a reduction in the value of the min-loss flow coefficient resulted in a reduction in the work coefficient. The difference is due to the presence of the inlet-to-exit radius ratio in equations three and four.

Performance maps were generated for the VIGV centrifugal compressor reported in Reference 6 . In this reference test data was reported for three IGV positions (-13°, 0°, 40°). The data as reported gives only the impeller performance. In order to generate a map of the impeller performance the program source was edited to eliminate the diffusser loss. The test data of Reference 6 was compared with the program results along the min-loss locus. These comparison plots are shown in Figures 19, 20, and 21. As can be seen from the plots as the IGV are closed, the flow is reduced and the impeller pressure rise increases. The agreement between the map and the test data is fairly good. According to Reference 6 , an additional loss of about 2.5% in impeller efficiency at the STP1 = 40° position occurred as a result of inlet flow distortion.

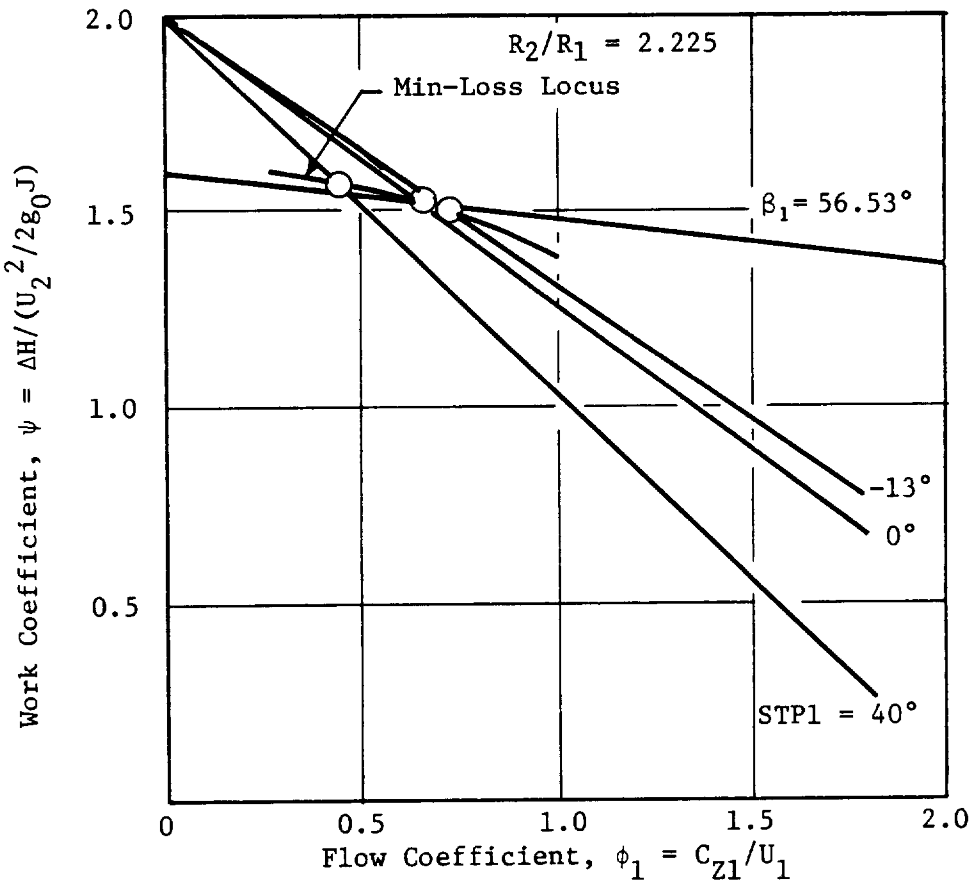

Figure 18. Stage Characteristic for VIGV (Centrifugal Compressor).

ORIGINAL PAGE IS
OF POOR QUALITY

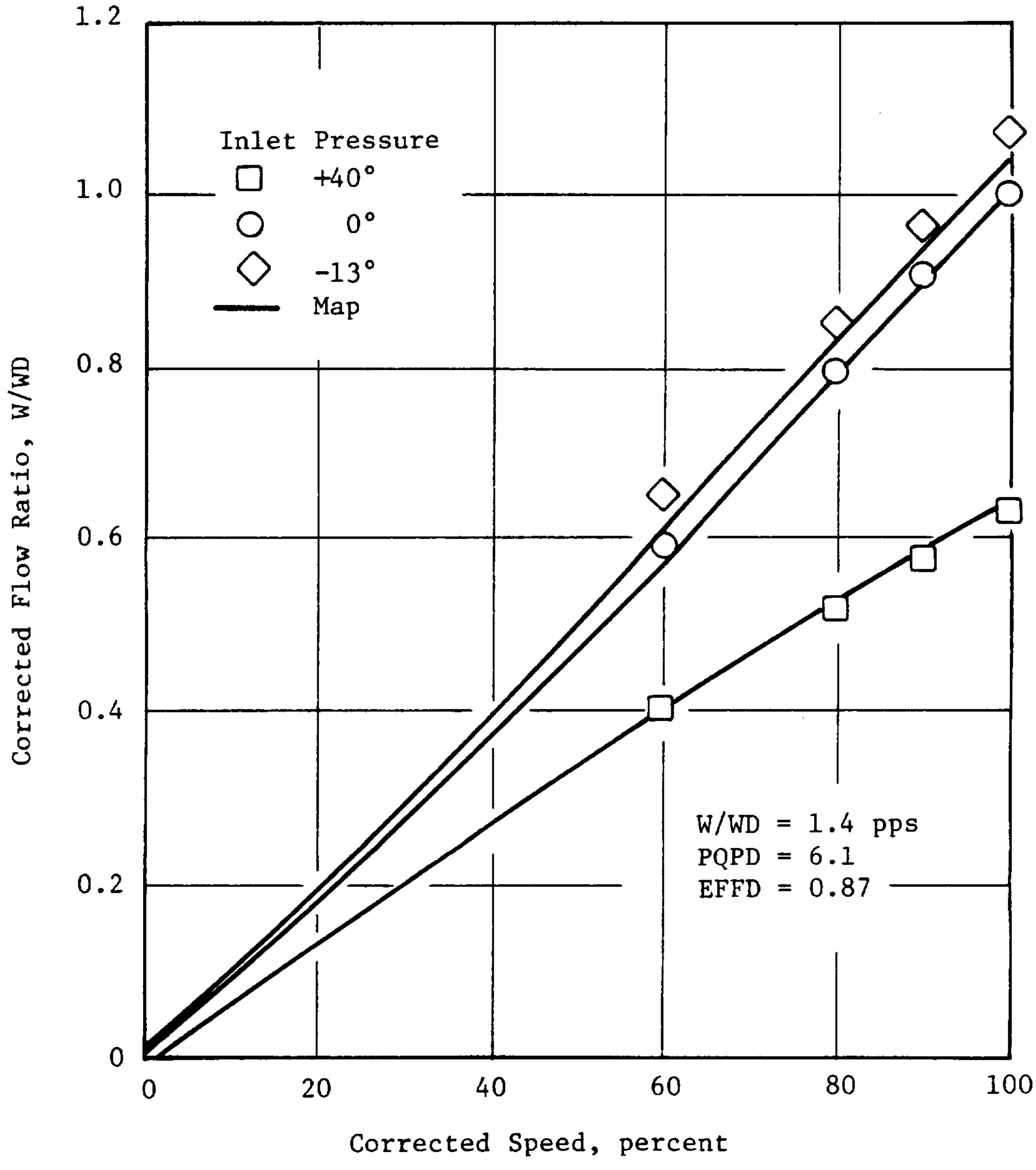

Figure 19. Flow Variation Along Min-Loss Locus (VIGV Centrifugal Compressor-Impeller Only).

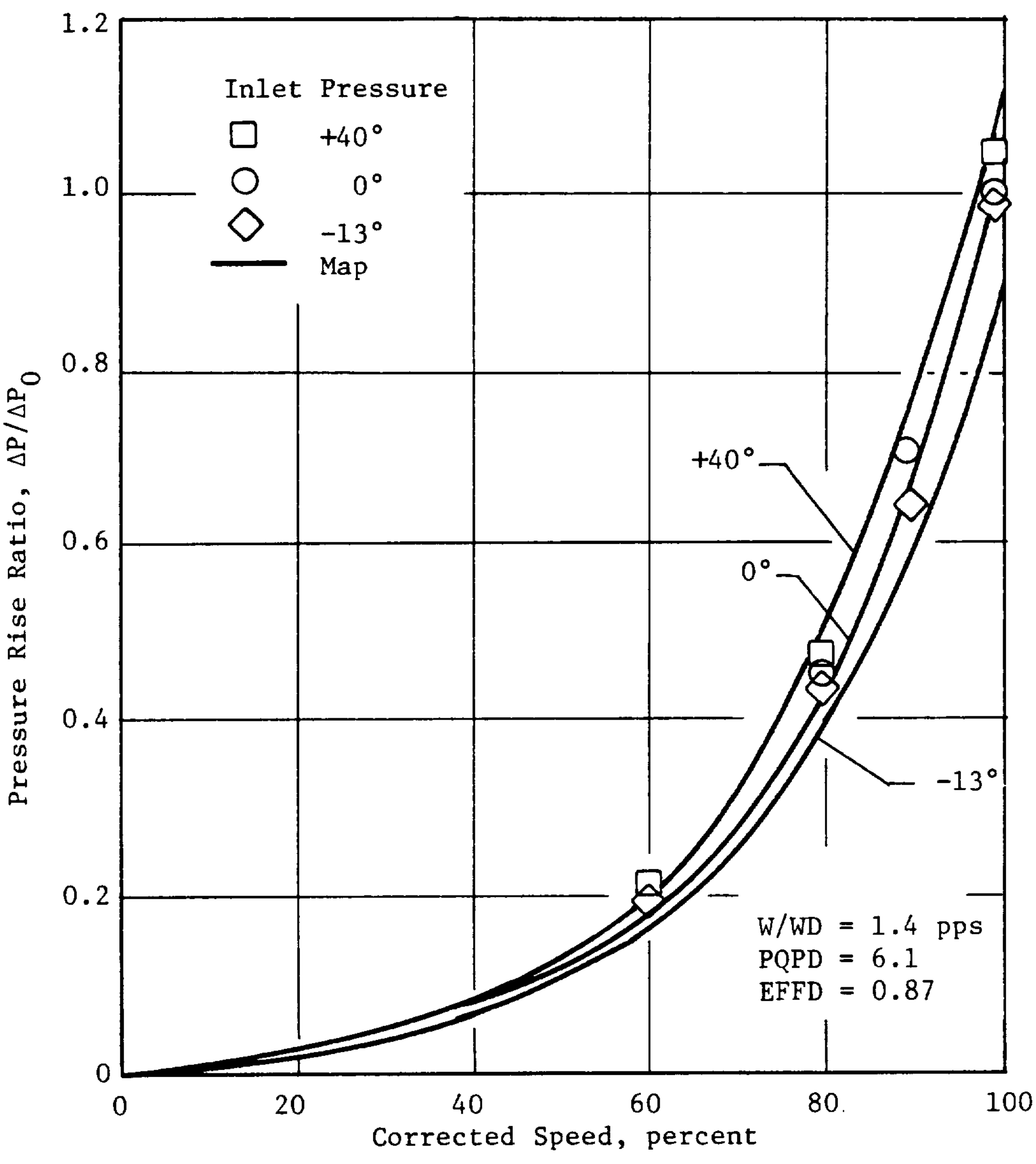

Figure 20. Pressure Rise Variation Along Min-Loss Locus (VIGV Centrifugal Compressor-Impeller Only).

ORIGINAL PAGE IS
OF POOR QUALITY

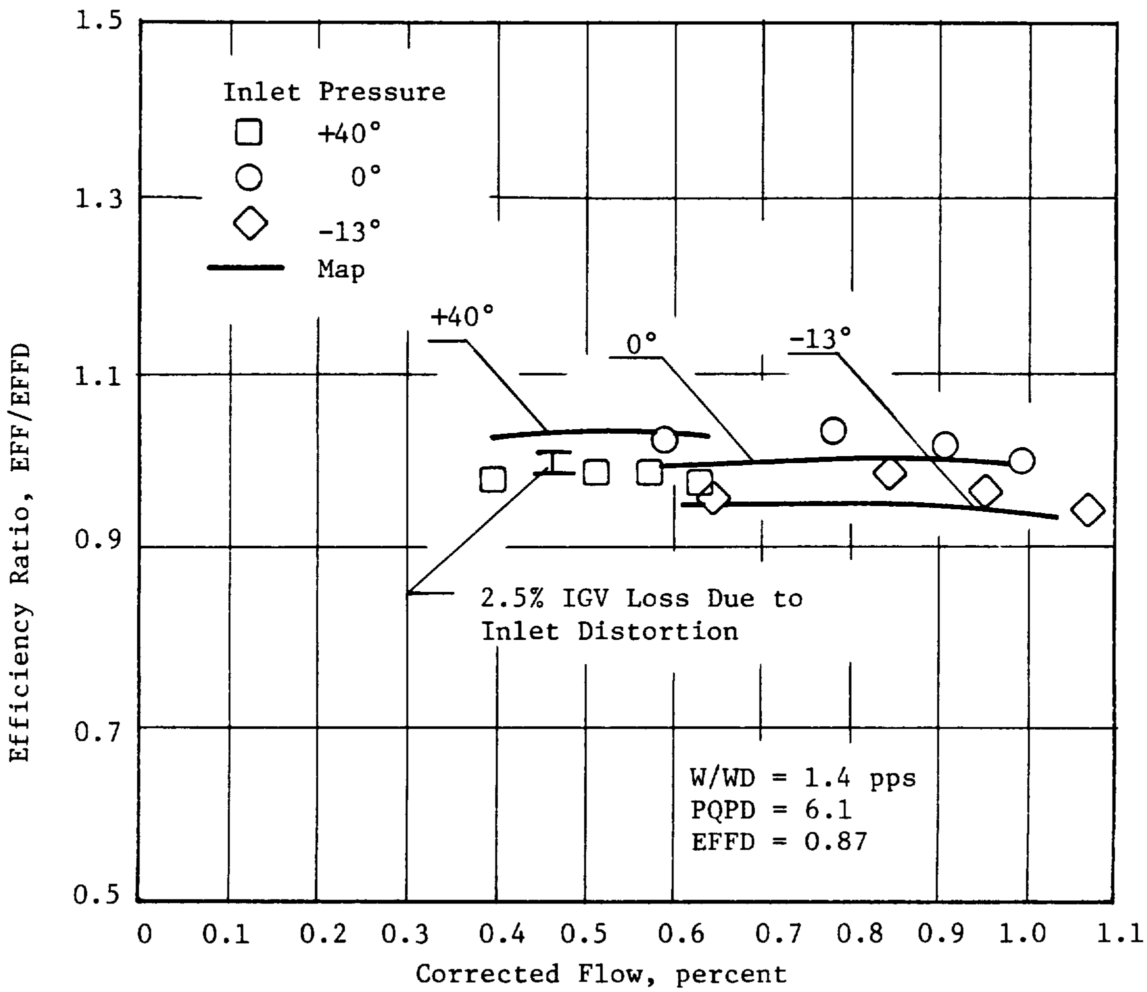

Figure 21. Efficiency Variation Along Min-Loss Line (VIDV Centrifugal Compressor-Impeller Only).

REFERENCES

1. Fishbach, Laurence H., and Caddy, Michael J., "NNEP: The Navy-NASA Engine Program," NASA TM X-71857, 1975.

2. Fishbach, Laurence H., "Konfig and Rekonfig - Two Interactive Pre-processing Programs to the NAVY/NASA Engine Program (NNEP)", NASA TMX-82636, May 1981.

3. Converse, G.L. and Giffin, R.G., "Extended Parametric Representation of Compressor Fans and Turbines", CMGEN User's Manual.

4. Bilwakesh, K.R., "Evaluation of Range and Distortion Tolerance for High Mach Number Transonic Fan Stages, Task II Stage Data and Performance Report for Undistorted Inlet Flow Testing," NASA CR-72787, January, 1971.

5. Rogers, C., "Typical Performance Characteristics for Gas Turbine Radial Compressors," Journal of Engineering for Power, Trans. ASME, Series A, Vol. 86., April 1964.

6. Rogers, C., "Impeller Stalling as Influenced by Diffusion Limitations," Journal of Fluids Engineering, Trans. ASME, March 1977.

DISTRIBUTION LIST - FINAL REPORTS - NAS3-23055

NASA Lewis Research Center
21000 Brookpark Road
Cleveland, OH 44135

Attn:

	Mail Stop	No. of Copies
Report Control Office	60-1	1
Library	60-3	3
M. J. Hartmann	3-7	1
L. W. Schopen	500-305	1
H. Mark	501-12	1
D. N. Bowditch	86-1	1
D. L. Nored	301-2	1
L. D. Nichols	60-2	1
C. L. Ball	60-5	2
L. E. Macioce	6-8	1
H. E. Rohlik	6-10	2
L. H. Fishbach	501-10	25

NASA Scientific and Technical Information Facility — 25
P.O. Box 875
Baltimore/Washington International Airport, MD 21240
Attn: Accessioning Department

DISTRIBUTION LIST (CONT'D)

One copy each to the following.

Mr. E. G. Blevins
AFWAL/POTA
Wright-Patterson AFB, OH 45433

Ms. Bobbye Ross
AiResearch Manufacturing
Company of Arizona
P.O. Box 5217
Phoenix, AZ 85010

Mr. Len Levine
AVCO-Lycoming Division
550 South Main Street
Stratford, CT 06497

Mr. Dushyant R. Arab
Senior Engineer
Propulsion - R&D
Beech Aircraft Corporation
Wichita, KS 67201

Mr. Erol Onat
The Boeing Company
P.O. Box 3999
Seattle, WA 98124

Mr. Paul W. Reisdorf
Technical Center
Caterpillar Tractor Co.
100 N. E. Adams Street
Peoria, IL 61629

Mr. Gerald W. White
Senior Propulsion Systems Analyst
Office of Scientific and Weapons Research
Central Intelligence Agency
Washington, DC 20505

Mr. Richard A. Sulkoske
Supervisor - Preliminary Design
Detroit Diesel Allison
P.O. Box 894
Indianapolis, IN 46206

Mr. Heiner O. Becker
Project Manager
Engineering Systems
Dresser Industries, Inc.
Dresser Computer Services Division
P.O. Box 796369
Dallas, TX 75379

Mr. M. A. Romano
Advanced Products
Fairchild Republic Company
Farmingdale LI, NY 11735

Mr. Lynn Marksberry
Fluidyne
5900 Olson Memorial Highway
Minneapolis, MN 55422

FTD/SDNP
Attn: M. A. Pennucci
Wright-Patterson AFB, OH 45433

Ms. Joyce R. Stinson, Manager
Systems Computations
Building 240G5
General Electric Co.
1000 Western Avenue
Lynn, MA 01910

Mr. Ronald E. Feddersen
Mail Stop C42-05
Grumman Aerospace Corporation
Bethpage, NY 11714

Mr. Ivan C. Oelrich
IDA/STD
1801 N. Beauregard Street
Alexandria, VA 22311

Mr. J. F. Stroud
Lockheed-California Company
Burbank, CA 91520

Mr. John C. Donohoe
Martin Marietta Aerospace
Mail Point 306
Orlando Division
P.O. Office Box 5837
Orlando, FL 32855

Eugene E. Covert, Sc.D.
Professor and Director
Department of Aeronautics and Astronautics
Center for Aerodynamic Studies
Massachusetts Institute of Technology
Cambridge, MA 02139

Dr. Robert T. Taussig
Director of Energy Technology
Mathematical Sciences North West, Inc.
2755 Northup Way
Bellevue, WA 98004

Mr. Donald C. Bingaman
McDonnell Douglas Corporation
271/C9A
P.O. Box 516
St. Louis, MO 63166

NASA Ames Research Center
237-11/Tom Galloway
Moffett Field, CA 94035

National Aeronautics and Space Administration
George C. Marshall Space Flight Center
Attn: PD31-78-41
Marshall Space Flight Center, AL 35812

NASA Langley Research Center
249/Shelby J. Morris
Hampton, VA 23665

Mr. Michael Caddy
Code 6052
Naval Air Development Center
Warminster, PA 18974

Mr. Paul Piscopo
Naval Air Propulsion Center
P.O. Box 7176
Trenton, NJ 08628

F. J. O'Brimski, Commander
Naval Air Systems Command
AIR-5284C2/JEL
Department of the Navy
Washington, DC 20361

Professor Thomas Houlihan
Code 69 HM
Naval Post Graduate School
Monterey, CA 93940

Mr. Andre By
Northern Research and Engineering Company
39 Olympia Avenue
Woburn, MA 01801

Mr. Arif Dhanidina, 3813/82
Propulsion Research
Northrop Aircraft Division
One Northrop Avenue
Hawthorn, CA 90250

Mr. Douglas Lee, 3828/52
Advanced Propulsion/Thermal Analysis
Northrop Aircraft Division
One Northrop Avenue
Hawthorn, CA 90250

Mr. Henry Snyder
Pratt & Whitney Aircraft Group
Engineering Computer Applications
Government Products Division, M/S 712-28
P.O. Box 2691
West Palm Beach, FL 33402

Mr. Robert Howlett
Pratt & Whitney Aircraft Division
400 Main Street
Mail Stop EB1F1
East Hartford, CT 06108

Mr. Larry Carroll
Propulsion Dynamics Inc.
2200 Somerville Road
Annapolis, MD 21401

Mr. William E. Flaus-D/71 B/6
North American Aircraft Division
Rockwell International
4300 East Fifth Avenue
P.O. Box 1259
Columbus, OH 43216

Mr. Larry Miller
Aerospace Marketing Manager
Rosemount Incorporated
P.O. Box 959
Burnsville, MN 55337

Mr. Nate Anderson
Mail Zone E-9
Solar Turbines International
P.O. Box 80966
San Diego, CA 92138

Professor I-Dee Chang
Department of Aeronautics and Astronautics
William F. Durand Building
Stanford University
Stanford, CA 94305

Mr. Mark A. Chappell
Sverdrup Technology Inc.
Mail Stop 500
Arnold Air Force Station, TN 37389

Mr. John J. Fox
Teledyne CAE
1330 Laskey Road
P.O. Box 6971
Toledo, OH 43612

Commander
US Army Aviation Research & Development
Command
Attn: DRDAV-DP/Dennis Enders
4300 Goodfellow Blvd.
St. Louis, MO 63120

Mr. Mike Galvis - DAVDL-ATL-ATP
Applied Technology Laboratory
U.S. Army Research Laboratory (AAVRADOM)
Fort Eustis, VA 23604

Dr. Paul C. Glance
Chief, Engine Function
Department of The Army
U.S. Army Tank-Automotive Research
and Development Command
Warren, MI 48090

Dr. Walter Obrien
Mechanical Engineering Dept.
Virginia Polytechnic Institute
Blacksburg, VA 24061

Dr. Reginald G. Mitchiner
Associate Professor of Mechanical Engineering
Virginia Polytechnic Institute and State
Univ.
Blacksburg, VA 24061

Mr. W. M. Rhoades
Manager, Propulsion and Thermodynamics
Vought Corporation
P.O. Box 225907
Dallas, TX 75265

Mr. Gerald J. Herman
Williams Research Corporation
2280 West Maple Road
Walled Lake, MI 48088